RMIT UNIVERSITY

# Transforming flexible devices to stretchable oxide-based electronics, photonics, and sensors

A thesis submitted in fulfilment of the requirements for the degree of Doctor of Philosophy

Philipp Gutruf, B.Eng.

School of Electrical and Computer Engineering
College of Science, Engineering and Health
RMIT University

October
2015

# Transforming flexible devices to stretchable oxide-based electronics, photonics, and sensors

Philipp Gutruf

(Doctor of Philosophy)

2015
RMIT University

# Declaration

I certify that except where due acknowledgement has been made, the work is that of the author alone; the work has not been submitted previously, in whole or in part, to qualify for any other academic award; the content of this thesis is the result of work which has been carried out since the official commencement date of the approved research program; any editorial work, paid or unpaid, carried out by a third party is acknowledged; and, ethics procedures and guidelines have been followed.

.....
Philipp Gutruf
Date: October 30, 2015

# Acknowledgements

This PhD would have not been possible without the help of many people inside and outside the lab. Many projects undertaken during my candidature where highly multidisciplinary, requiring input from colleagues and collaborators.

First and foremost, I would like to thank my first supervisors Dr. Sharath Sriram and Dr. Madhu Bhaskaran who provided me with an excellent platform and resources to undertake this PhD. I would like to especially thank them for their patience, trust and encouragement to engage in activities outside the lab such as overseas research visits, media work, competitions and seminars. Your encompassing guidance is greatly appreciated.

Secondly I would like to thank my second supervisor Dr. Sumeet Walia for his help with many projects and especially for his readily availability.

I would like to express my gratitude towards RMIT Unversity, with its facilities, Micro Nano Research facility (MNRF), Microelectronics and Materials Technology Centre (MMTC) and the RMIT Microscopy and Microanalysis Facility (RMMF) for providing me with facilities to undertake this Ph.D program. I also wish to thank the Department of Education, Science, and Training of the Australian government for the International Postgraduate Research Scholarship.

Furthermore I would also like to thank Prof. John A Rogers for giving me the opportunity to work with his group at University of Illinois at Urbana–Champaign (UIUC).

For a great work environment, collaborations and scientific input I would like to thank my co-workers at RMIT University Dr. Eike Zeller, Dr. Hussein Nili, Dr. Sivacarendran Balendhran, Dr. Mahyar Nasabi, Dr. Tristan Crasto and Geeth Devendra. Furthermore I would like to thank collaborators at the University of Adelaide, Prof. Christophe Fumeaux, Dr. Withawat Withayachumnankul and Chengjun Zou and at the University of Illinois at Urbana–Champaign Dr. Jeonghyun Kim and Tony Banks.

I also would like to thank the technical staff Yuxun Cao, Phil Francis, Chi Ping Wu and Paul Jones for their support with various equipment.

Furthermore I would like to thank my friends outside the University and my family, especially my parents for supporting my academic career and providing me with the opportunity and encouraging me to undertake many extracurricular opportunities that shaped my skills outside of academic institutions.

Lastly I would like to thank my fiancé, my love and best friend, Kate Horrack for her unconditional support during the many hours of work, kindness and loving nature while undertaking her PhD at the same time.

# Abstract

Lightweight compact electronics are currently the most popular personal electronic devices. A trend towards wearable and body compatible smart devices is clearly indicated, creating the demand for electronics to be fully flexible and stretchable to realise next generation devices.

To allow for this additional degree of freedom, strategies for fabricating these devices need to be established. The fabrication of such devices pose a challenge to materials science due to the inherent brittle nature of metals, oxides and semiconductors, the core building block for powerful electronics. This thesis explores new methods of integrating these materials into flexible and stretchable platforms.

Initially a comprehensive study into metal films on flexible substrates is carried out with insights into strategies to reduce the sensitivity towards strain. Based on these insights, multilayer resonating terahertz structures on a flexible platform are presented and analysed, showcasing the ability to distinguish polarisation efficiently.

The integration of a functional material namely zinc oxide into a flexible platform is demonstrated by realising a visible-blind UV imaging array capable of operating in various bending states.

In order to enable an additional degree of freedom, strategies to enable stretchability of functional oxides is explored. A novel method of transferring high temperature processed oxides (indium tin oxide) is presented, to overcome process temperature limitations. Secondly, a phenomena named “micro-tectonics” which allows oxides to stretch and bend is discovered and analysed.

Based on the micro-tectonic effect zinc oxide stretchable devices are demonstrated that are capable of detecting UV and gases efficiently at room temperature which outperform their rigid counterparts.

Additionally high refractive index contrast devices are shown that dynamically manipulate visible light via device deformation. Multifaceted analysis provides insight into the excellent tunability of these diffractive and resonating optical devices.

The thesis offers a cross-disciplinary insight into incorporation of functional oxide thin films with flexible and stretchable materials, and the potential for a new paradigm of functional devices.

# Contents

**DECLARATION** ..... **III**

**ACKNOWLEDGEMENTS** ..... **IV**

**ABSTRACT** ..... **V**

**CONTENTS** ..... **VI**

**INTRODUCTION** ..... **2**

1.1 Preface ..... 2

1.2 Motivation and Thesis Outline ..... 2

1.2.1 Motivation ..... 2

1.3 Integration of Functional Films in Flexible and Stretchable Platforms – Current Progress and Perspective in Flexible and Stretchable Electronics ..... 3

1.3.1 Introduction ..... 3

1.3.2.1 Direct Deposition ..... 4

1.3.2.2 Transfer Techniques ..... 5

1.3.3 Applications ..... 6

1.3.3.1 Flexible Electronics ..... 6

1.3.3.2 Stretchable Electronics ..... 7

1.3.4 Perspective ..... 7

1.4 Publications and Recognition ..... 9

1.4.1 Journal Publications ..... 9

1.4.2 Conference Contributions ..... 10

1.5 Original Scientific Contributions ..... 11

**FLEXIBLE METAL BASED DEVICES** ..... **12**

2.1 Strain Response of Stretchable Micro-Electrodes: Controlling Sensitivity With Serpentine Designs and Encapsulation ..... 12

2.2 Flexible Bi-layer Terahertz Chiral Metamaterials ..... 13

**FLEXIBLE MULTILAYER OXIDE BASED DEVICE** ..... **14**

3.1 Flexible Visible Blind Imaging Device enabled by Oxygen Deficient Zinc Oxide Sensing Elements ..... 14

**INCORPORATION OF HIGH TEMPERATURE PROCESSED OXIDES FOR STRETCHABLE ELECTRONICS** ..... **15**

4.1 Transparent Functional Oxide Stretchable Electronics: Micro-Tectonics Enabled High Strain Electrodes ..... 15

**STRETCHABLE ZINC OXIDE BASED DEVICES ..... 16**

5.1 Stretchable and Tunable Microtectonic ZnO-Based Sensors and Photonics. ..... 16

**STRETCHABLE PHOTONICS: GRATINGS AND RESONANT STRUCTURES ..... 17**

6.1 Mechanically Tunable High Refractive Index Contrast $TiO_2$–PDMS Gratings ..... 17

6.2 Mechanically Tunable Dielectric Resonator Metasurfaces at Visible Frequencies ..... 18

**CONCLUSION AND FUTURE WORK ..... 19**

7.1 Conclusion ..... 19

7.2 Outlook ..... 19

**REFERENCES ..... 21**

**APPENDIX ..... 25**

7.3 Supplementary Information for Chapter 2.1 ..... 26

7.4 Supplementary Information for Chapter 3.1 ..... 29

7.5 Supplementary Information for Chapter 4.1 ..... 41

7.6 Supplementary Information for Chapter 5.1 ..... 45

7.7 Supplementary Information for Chapter 6.1 ..... 58

7.8 Supplementary Information for Chapter 6.2 ..... 64

# Introduction

## 1.1 Preface

This thesis has been prepared for the submission as thesis with publications according to the guidelines provided by the School of Electrical and Computer Engineering.

## 1.2 Motivation and Thesis Outline

### 1.2.1 Motivation

The way we interact with our electronic devices has changed significantly over the past decade. Increasingly we move away from stationary devices, such as desk top computers, to more portable and versatile gadgets such as laptops, tablets, smartphones and recently wearable devices such as smart wristbands or smart watches. Hence, a trend towards light weight portable devices that integrate with the human body is clearly indicated.

Current commercial wearable devices make use of standard electronic parts in a new package, which is designed to accommodate flexibility, such as a wrist band, to form a flexible electronic device. However great effort is directed towards next generation devices that allow for full flexibility and stretchability. Such devices will give a new degree of freedom, enabling novel applications such as body mounted electronics.

The main challenge to make such fully flexible and stretchable devices is the integration of functional materials such as metals and oxides into a flexible platform, such as thin plastic sheets, or a stretchable platform, such as elastomeric materials. Firstly a mechanism or strategy needs to be established to enable the oxide to stretch and bend, secondly the temperature limits of the organic substrate need to be respected. Both are fundamental problems that require detailed attention to make a fully stretchable device feasible.

This thesis is directed towards the exploration of new methods of integrating oxides into flexible and stretchable platforms, and showcase the capabilities of such devices.

## 1.3 Integration of Functional Films in Flexible and Stretchable Platforms – Current Progress and Perspective in Flexible and Stretchable Electronics

### 1.3.1 Introduction

The capabilities of fully flexible and stretchable electronic devices have been demonstrated over the recent years with many researchers focussing their efforts on these devices. The academic success of the concept of electronics that can stretch and bend has been accompanied by increasing interest of industry with commercial devices such as flexible fitness tracker, radio-frequency identification (RFID) patches and rollable keyboards which are already available on the consumer market. Commercial devices use conventional electronic components in a flexible housing to allow for state of the art functionality whilst maintaining the advantages of a highly lightweight and adaptable device. Academic research however, focuses on finding solutions on how to create electronics that have as little as possible rigid components to allow for devices that can adapt seamlessly to curvilinear surfaces.

The curvilinear adaptability offers distinct advantage over conventional rigid electronic devices. Firstly such devices can adapt seamlessly to the human body, which allows for excellent vital information collection through intimate contact with the skin or organs and almost unnoticeable integration with the host. Therefore such form of electronic device is highly advantageous for biomedical device.

Secondly such mechanically deformable devices allow for a new freedom in device design allowing for mechanically tunable devices paving the way for fundamentally new applications. Mechanical deformability can be in form of flexibility or stretchability. Flexible devices are able to bend allowing them to wrap around objects or adapt to surfaces. Stretchable devices have the additional ability to deform with an object allowing for an extra degree of freedom.

The realisation of such devices can be accomplished via fundamentally different synthesis routes. One of the most obvious synthesis routes is to use organic materials that are intrinsically flexible or stretchable. The use of functional organic materials avoids the integration of brittle materials such as silicon or functional oxides. This allows for the resulting devices to be highly stretchable[1]. Devices such as large area stretchable Light Emitting Diodes (LED)´s [2], solar cells[3], pressure sensors[4], memory[5] and transistor arrays[6] could be demonstrated. Additionally to such applications organic stretchable and flexible electronics are highly roughed[7] and allow the ability of integration of self-healing materials[8]. However such a purely organic synthesis approach also has the downsides of degradation through ambient oxygen[9] and the performance of the organic functional materials generally lacks behind its traditional semiconductor and oxide materials[10]. Furthermore the patternability of such organic device is limited, allowing only demonstration of large area devices which results in a fundamental scaling problem which limits the use of these synthesis techniques for low integration density devices only.

Another approach is to combine the advantages of mechanical durability of organic devices with the high performance nature of semiconductors and functional oxides. The mechanical stretchability of these intrinsically brittle materials is created by forming a network of small elements loosely connected to each other resulting in a net stretchability[11]. This technique is often applied to materials such as nano-wires by mixing these functional element into an elastomeric binder resulting in a highly performing stretchable device[12]. Devices such as energy harvesters[13], gas sensors[14], radio frequency (RF)-antennas[15] and ultra violet (UV)-sensors[16]. A similar concept is employed with nano particles which leads to comparable results, devices such as stretchable RF-antennas[17], hydrogen sensors[18], super capacitors[19] and pressure sensors[20]. One of the main advantages of such nanoparticle based devices is that they are potentially printable[21] allowing for rapid prototyping stretchable devices as well as facile manufacturing. However the feature size provided by printing is orders of magnitudes bigger than contemporary micro and nano fabrication which makes this technique only suitable for low integration densities in comparison to rigid electronics.

Lastly the approach that this introduction and thesis focuses on, is the adaptation of conventional electronic devices, fabricated with conventional micro and nano fabrication techniques onto a stretchable or flexible platform. This synthesis route offers the distinct advantage of using well established methods and theories to create highly performing devices with high integration densities. However the intrinsically brittle nature of the key materials such as semiconductors and functional oxides poses a distinct mechanical challenge requiring new insights into how such materials behave on flexible and stretchable platforms.

### 1.3.2 Fabrication Methods

In order to create such mechanically deformable devices, the fundamental mismatch of stretchable and flexible materials, which are mostly organic, and intrinsically hard and brittle materials such as oxides and semiconductors that often define the functionality, need to be overcome. In addition to the mechanical incompatibilities, fabrication temperatures pose another fundamental problem. While organic materials such as elastomers and plastics which form the base for mechanically deformable devices are usually processed at temperatures of lower than 200 degrees Celsius, oxides and semiconductors often require process temperatures in excess of 400 degrees Celsius. Such high temperatures usually lead to decomposition of organic materials making a bottom up fabrication approach for some applications not feasible.

In order to overcome these problems various strategies have been proposed. Often the synthesis route is specific to the individual device while other more general approaches are reported more frequently.

#### 1.3.2.1 Direct Deposition

One of the most common synthesis strategies is the direct deposition method. Direct deposition is a fabrication strategy mostly employed for room temperature deposited layers such as metal films to form

conductors and oxides processed at room temperature where a crystalline growth is not essential to the function and performance of the device.

The use of elastomeric films as a substrate to form a stretchable electronic device typically do not allow for a high stretchability. In the case of a metallised elastomer, typically polydimethylsiloxane (PDMS), forming a stretchable conductor, results in a usable stretchability of around 10% in case of the extensively studied gold thin films[22-24]. Such films endure repeated stretchability and increase their resistance with strain, largely governed by their failure mechanism called micro-cracking. Micro-cracking occurs in well adhered thin films to elastomeric materials[25] and leads to an effective reduction in conductor cross-section with increasing strain by the formation of nano islands[26]. Such an effect can also be observed in plastically deformable materials such as polyimide[27]. In order to increase stretchability various strategy can be employed such as pre-straining the elastomeric materials before direct deposition which causes the thin film to wrinkle, leading to an improved stretchability by the amount of pre-strain induced[28].

However one of the most prevalent problems with direct deposition is thermally induced shrinkage and expansion and finally destruction of the elastomeric or plastic substrate. Thermal expansion especially applies to elastomeric materials, having a high thermal expansion coefficient, making direct deposition synthesis especially difficult[29]. Therefore thermally stable but mechanically flexible materials such as polyimide are popular candidates to fabricate flexible and highly integrated devices with elevated synthesis temperatures[30].

#### 1.3.2.2 Transfer Techniques

In order to overcome thermal expansion problems as well as synthesis temperature limitations and surface properties such as the hydrophobic nature of elastomeric substrates, a technique is required where the device is prepared on a temporary substrate which can withstand the synthesis conditions and then transferred onto the flexible or stretchable target substrate.

A simple example of such a temporary substrate is conversely the use of an elastomeric substrate as a temporary host. This technique overcomes the problem of the hydrophobic nature of elastomeric substrates. The polymer layer is externally prepared and metallised and subsequently hand laminated to the elastomer substrate. Therefore the wettability issues are surpassed allowing for the creation of ultrathin flexible electronics[31].

The technique can also be used in order to enable highly stretchable electronics by preparing the device and subsequently bonding it to a highly stretchable elastomer such as Ecoflex, additional mechanical strength and stretchability can be introduced with a so called mutual mechanical plane where the functional material is sandwiched between polyimide and pre-patterned serpentine designs[32], this leads to an unfolding of the serpentine structure with no large strain subjected to the functional layer[33]. With this technique devices with a stretchability of up to 300% can be achieved[34].

A synthesis technique for a bottom up fabrication approach is the use of a sacrificial layer, such a layer is introduced at the start and is selectively removed when the fabrication is completed, freeing the layers above resulting in a freestanding device that can be either supported by an elastomeric or plastic substrate or directly printed onto curvilinear surfaces. This technique offers high design freedom and little issue with thermal expansion and topological roughness which are crucial for a high resolution fabrication for high integration density devices.

Sacrificial layers have to be chosen very carefully, they have to be selective to the device materials and are therefore often exotic materials such as poly vinyl alcohol (PVA)[35] which is water dissolvable, conversely this means that the device fabrication cannot involve water based chemicals.

More commonly used sacrificial layers are oxides. These sacrificial layers offer the key benefit of being highly temperature resistant and are therefore the synthesis method of choice for semiconductor based device such as transistors that often have to be doped and annealed at temperatures close to 1000 °C[36]. These sacrificial layers are often just placed directly under the device with openings in order to facilitate a quick and selective dissolution[37], and hence large area continuous device are very hard to fabricate.

Another hurdle when using a sacrificial layer is that the device has to be designed upside down with a subsequent lift of the temporary substrate making the use of conventional micro-fabrication techniques hard. This problem can be solved by a popular technique called transfer printing. Here, an elastomeric stamp is used in order to pick up a device from a temporary substrate and subsequently placed onto the final host substrate[38].

Lastly, metal films can also be used to develop an effective transfer method, this technique is extensively investigated in this thesis and is demonstrated to offer a ubiquitous platform to perform high resolution transfer.

### 1.3.3 Applications

The possibilities provided by the integration of oxides and semiconductors into a flexible platform are multifaceted and are not restricted to the creation of electronic devices with advanced capabilities. This integration also offers a platform for advances in other areas of research such as optics and photonics. Additionally, the ability to stretch and bend thin films in a controlled manner allows for scientific insight into the makeup and behaviour of materials and therefore forms an excellent scientific tool to study thin film behaviour.

#### 1.3.3.1 Flexible Electronics

As discussed in the fabrication section 1.3.2, flexible plastics such as polyimide and polyethylene terephthalate (PET) offer a good base for flexible electronics with high integration density, multilayer designs and highly complex devices. Devices based on the highly temperature and chemically stable

substrate polyimide have already been demonstrated with highly unique capabilities that surpass the opportunities offered by conventional rigid electronics. Examples for such devices that are somewhat body compatible are piezoelectric generators that can operate in the proximity of a bovine lung and heart generating power for pacemakers[39] and injectable ontogenetic needles for drugless pain reduction[40]. Furthermore complex devices such as imaging which are discussed in chapter 3.1, transistor arrays for in vivo brain activity recording[41], flexible diagnostic platform for virus detection[42] and flexible antenna devices ranging from radio [43] to terahertz frequency[44] which is also investigated in chapter 2.2. Furthermore substrates such as the cheap and widely available PET are transparent and therefore suitable for fully transparent devices. PET is widely used to create, imperceptible magnetoelectronics[45], transparent and flexible transistors[46] and solar cells[47]. Additionally to these devices, flexible platforms are widely used to induce strain in for in situ measurements such as the study of piezoelectric nanowires [48], piezotronic effect in ZnO nanowires[49] and transport properties of semiconductors[50]

#### 1.3.3.2 Stretchable Electronics

The opportunities provided by stretchable electronics allow for electronics that are mounted onto an elastomeric substrate or biological tissue allowing for powerful applications enabling functionalities only associated with stretchable electronics[37]. Especially *in vitro* applications benefit from a stretchable device form, applications such as electronics mounted on an inflatable catheter[51], membranes for *in vitro* cardiac electro therapy[52] and *in vitro* pH sensing[53]. The opportunities provided by skin mounted, also called epidermal, devices allowed for multifaceted opportunities for consumer applications such as passive wearable near filed communication (NFC) tags[31,54], sensing applications such as strain and electrophysical parameters[55] and the two-dimensional determination of modulus allowing for skin disease diagnosis[56]. The stretchability of the devices also allows for integration with clothes enabling electronic textiles[57] and allowing for smart packaging of stretchable electronics[58].

### 1.3.4 Perspective

Mechanically deformable devices offer opportunities allowing for a possible evolution in functionality and the way we interact with smart devices. The rapidly evolving field of flexible and stretchable electronics providing a platform for advancements across research fields from biology over electronics to chemistry and physics is suggesting science fiction like devices in the near future. This becomes evident by the vast demonstration of novel devices in the past years in academic research and the enormous commercial interest and heavy investment especially in facilities solely for the porpoise of advancing flexible electronics. The success of flexible electronics will rely on the advancement of key fabrication strategies such as high temperature processed oxides and semiconductors into flexible and stretchable platforms which are extensively discussed in this thesis.

### 1.3.5 Thesis Structure

This thesis is focussing on the key problems identified in the introduction to advance the field of stretchable and flexible electronics.

Initially a comprehensive study into metal films on flexible substrates is carried out with insights into strategies to reduce the sensitivity of flexible electrodes towards strain.

Based on the insights gained from the metal thin film study, flexible multilayer resonating terahertz structures are presented and analysed. Such structures show the ability to distinguish polarisation efficiently due to the low loss nature of the flexible substrate.

To advance functionality of these flexible devices, the integration of functional oxides is employed to allow for flexible large-area visible-blind UV imaging arrays tolerant to curvature**.** The functionality is enabled by crystalline oxygen-deficient zinc oxide pixels, which show high sensitivity and fast response to UV light.

In order to evolve the functionality from flexible to stretchable devices two of the key issues in the creation of stretchable electronics are addressed. Firstly a novel method of transferring high temperature processed oxides, namely indium tin oxide (ITO) is presented, to overcome process temperature limitations. Secondly, a phenomenon named “micro-tectonics” is discovered and the ability of such a surface structure to form a fully stretchable oxide layer is described and explored.

Based on the newly discovered micro-tectonic surface, oxygen deficient zinc oxide sensors capable of detecting gases at room temperature and UV radiation are presented. These fully stretchable sensors are directly compared to their rigid counterparts and demonstrate to be more sensitive due to the micro-tectonic surface structure. Furthermore optical devices such as oxide based mechanically tuneable gratings are shown exploiting the high resolution capability of the novel transfer technique.

Additional insight into such mechanically tunable optics is provided by the investigation of titanium dioxide tunable gratings via *in situ* characterisation techniques backed by finite element analysis giving insight into the mechanical behaviour of hard high modulus features an elastomeric matrix under strain.

Building on these studies, tunable resonators operating at visible frequencies are proposed, fabricated, tested and analysed using optical and mechanical finite element simulation offering a unique insight into the working principles of such a device.

## 1.4 Publications and Recognition

The author has published extensively, resulting in 14 journal publications with 6 as a first author with an average impact factor of 9.26, during his candidature. Not all work that the author published during his candidature is represented in this thesis. Notable work that is not discussed here is the collaboration with the Rogers group, resulting in two high impact publications in the journals of *Advanced Functional Materials* and *Small* covering the topic of body mounted electronics. Furthermore, work originated from an extensive collaboration with the University of Adelaide is partially presented in this thesis.

The publications relevant to this thesis are marked with an asterisk and are displayed in the order of appearance in the thesis.

### 1.4.1 Journal Publications

1. ***P Gutruf,** S Walia, M Nur Ali, S Sriram, and M Bhaskaran "Strain response of stretchable micro-electrodes: Controlling sensitivity with serpentine designs and encapsulation" *Applied Physics Letters* 104, 2, 021908 (2014).
   Impact factor: 3.569 JCR rank: 21/143 in Applied Physics category

2. *A Sonsilphong, **P Gutruf,** W Withayachumnankul, D Abbott, M Bhaskaran, S Sriram and N Wongkasem "Flexible bi-layer terahertz chiral metamaterials" *Journal of Optics* 17, 8, 085101 (2015).
   Impact factor: 1.887 JCR rank: 25/86 in Optics category

*3.* ***P. Gutruf,** S.Walia, M. Bhaskaran and S. Sriram "Flexible visible blind imaging device enabled by oxygen deficient zinc oxide sensing elements" in press *Advanced Electronic Materials* (2015) DOI: 10.1002/aelm.201500264
   Impact factor: TBA JCR rank: TBA

4. ***P Gutruf**, C M Shah, S Walia, H Nili, A S Zoolfakar, C Karnutsch, K Kalantar-zadeh, S Sriram, M Bhaskaran "Transparent functional oxide stretchable electronics: Micro-tectonics enabled high strain electrodes" *NPG Asia Materials*, 5, 9, e62 (2013).
   Impact factor: 11.347 JCR rank: 14/259 in Materials Science, Multidisciplinary category

5. ***P Gutruf**, E Zeller, S Walia, H Nili, S Sriram, and M Bhaskaran. "Stretchable and Tunable Microtectonic ZnO-Based Sensors and Photonics." *Small, 11, 35,* 906-912 (2015).
   Impact factor: 8.646 JCR rank: 16/259 in Materials Science, Multidisciplinary category

*6.* ***P Gutruf**, E Zeller, S Walia, S Sriram and M Bhaskaran "Mechanically Tunable High Refractive Index Contrast $TiO_2$–PDMS Gratings" *Advanced Optical Materials,* 3, 11, 1565-1569 (2015).
   Impact factor: 4.063 JCR rank: 7/86 in Optics category

*7.* ***P Gutruf**, C Zou, W Withayachumnankul, M Bhaskaran, S Sriram and C Fumeaux "Mechanically Tunable Dielectric Resonator Antennas at Visible Frequencies" *ACS Nano,* Article ASAP (2015) DOI: 10.1021/acsnano.5b05954
   Impact factor: 14.412 JCR rank: 10/259 in Materials Science, Multidisciplinary category

8. J Kim, A Banks, Z Xie, S Y Heo, **P Gutruf** , J W Lee, S Xu, K I Jang, F Liu, G Brown, J Choi, J H Kim, X Feng, Y Huang, U Paik, and J A Rogers ,Miniaturized Flexible Electronic Systems with Wireless Power and Near-Field Communication Capabilities. *Advanced Functional Materials, 25, 30,* 4761-4767 (2015)
   Impact factor: 12.311 JCR rank: 12/259 in Materials Science, Multidisciplinary category

9. J Kim, A Banks, H Cheng, Z Xie, S Xu, K Jang, J W Lee, Z Liu, **P Gutruf**, X Huang, P Wei, F Liu, K Li, M Dalal, R Ghaffari, X Xeng, Y Huang, S Gupta, U Paik and J A Rogers "Epidermal Electronics with Advanced Capabilities in Near-Field Communication" *Small*, 11, 8, 906-912 (2015).
   Impact factor: 8.646 JCR rank: 16/259 in Materials Science, Multidisciplinary category

10. S Walia, M Shah, **P Gutruf**, H Nili, D R Chowdhury, W Withayachumnankul, M Bhaskaran and S Sriram " Flexible metasurfaces and metamaterials: A review of materials and fabrication processes at micro- and nano-scales" *Applied Physics Reviews,* 2, 1, 011303 (2015).
    Impact factor: TBA JCR rank: TBA

11. H Nili, S Walia, A E Kandjani, R Ramanathan, **P Gutruf**, T Ahmed, S Balendhran, V Bansal, D B Strukov, O Kavehei, M Bhaskaran and S Sriram "Donor-Induced Performance Tuning of Amorphous $SrTiO_3$ Memristive Nanodevices: Multistate Resistive Switching and Mechanical Tunability." *Advanced Functional Materials,* 25, 21, 3172–3182 (2015).
    Impact factor: 12.311 JCR rank: 12/259 in Materials Science, Multidisciplinary category

12. T Niu, W Withayachumnankul, A Upadhyay, **P Gutruf**, D Abbott, M Bhaskaran, S Sriram, and C Fumeaux "Terahertz reflectarray as a polarizing beam splitter" *Optics Express*, 22, 13, 16148-16160 (2014)
    Impact factor: 3.499 JCR rank: 8/86 in Optics category

13. D Headland, S Nirantar, W Withayachumnankul, **P Gutruf**, D Abbott, M Bhaskaran, C Fumeaux and S Sriram "Terahertz Magnetic Mirror Realized with Dielectric Resonator Antennas" *Advanced Materials* 27, 44, 7137-7144 (2015)
    Impact factor: 18.172 JCR rank: 4/259 in Materials Science, Multidisciplinary category

14. W. S.Y. Wong, **P Gutruf**, S Sriram, M Bhaskaran, Z Wang and A Tricoli "Strain Engineering of Wave-like Nanofibers for Dynamically Switchable Adhesive/Repulsive Surfaces" *Advanced Functional Materials* in press DOI: 10.1002/adfm.201503982
    Impact factor: 12.311 JCR rank: 12/259 in Materials Science, Multidisciplinary category

### 1.4.2 Conference Contributions

The author participated in various conferences and meetings worldwide in his candidature, presenting the work discussed in this thesis.

1. **P Gutruf**, S Walia, C M Shah, S Sriram, and M Bhaskaran "Micro-tectonics enabled stretchable transparent oxide electrodes" E-MRS Spring Meeting (2015)

2. **P Gutruf**, S Walia, E Zeller, S Sriram and M Bhaskaran "Stretchable room temperature ZnO sensors" E-MRS Spring Meeting (2015)

3. **P Gutruf**, C M Shah, S Walia, H Nili, A S Zoolfakar, K Kalantar-zadeh, S Sriram and M Bhaskaran "Solving the process temperature problem for flexible electronics – high quality oxide transfer to elastomers" 56th Electronic Materials Conference EMC (2014)

4. **P Gutruf**, M Bhaskaran, S Sriram "Flexible and Stretchable Electronics with High Temperature Oxides" Nano and Giga Challenges in Electronics, Photonics and Renewable Energy (2014)

5. **P Gutruf**, C M Shah, S Walia, H N Ahmadabadi, A S Zoolfakar, C Karnutsch, K Kalantar-Zadeh, S Sriram, M Bhaskaran "A novel transfer process for high temperature oxides stretchable electronics" SPIE Micro+Nano Materials, Devices, and Applications (2013)

6. **P Gutruf**, C M Shah, S Walia, A S Zoolfakar, K Kalantar-zadeh, S Sriram & M Bhaskaran "Nano-overlapped tectonic plates enabled high temperature oxide stretchable electronics" ANN Early Career Workshop (2013)

7. H N Ahmadabadi, **P Gutruf**, K Kalantar-Zadeh, M Bhaskaran, S Sriram "Conduction mechanisms and resistive switching in RF magnetron sputtered $SrTiO_3$ epitaxial ultra-thin films and multilayer structures" SPIE Micro+Nano Materials, Devices, and Applications (2013)

## 1.5 Original Scientific Contributions

- Flexible electronics with strain tolerant electrode designs and aligned multilayer structures for electronic, photonic, and sensing applications
- Novel transfer technique to combine high temperature oxides with elastomers unlocking devices with full range of functionalities, while creating insight into micro-scale mechanics of plate-like oxides
- Utilising micro-tectonic oxygen-deficient oxides to enhance carrier concentration and surface area, and thereby, enable higher sensitivity devices and significant room temperature performance
- High resolution dielectric patterns embedded in an elastomeric matrix enabling efficient, tunable optical devices: Gratings and resonators

# Flexible Metal Based Devices

## 2.1 Strain Response of Stretchable Micro-Electrodes: Controlling Sensitivity With Serpentine Designs and Encapsulation

The work related to this Chapter has been peer-reviewed and published in *Applied Physics Letters*.

The full paper can be obtained via http://dx.doi.org/10.1063/1.4862264

This work can be cited as: **P Gutruf,** S Walia, M Nur Ali, S Sriram, and M Bhaskaran "Strain response of stretchable micro-electrodes: Controlling sensitivity with serpentine designs and encapsulation" *Applied Physics Letters* 104, 2, 021908 (2014).

## 2.2 Flexible Bi-layer Terahertz Chiral Metamaterials

The work related to this Chapter has been peer-reviewed and published in *Journal of Optics*.

The full paper can be obtained via http://dx.doi.org/10.1088/2040-8978/17/8/085101

This work can be cited as: A Sonsilphong, **P Gutruf,** W Withayachumnankul, D Abbott, M Bhaskaran, S Sriram and N Wongkasem "Flexible bi-layer terahertz chiral metamaterials" *Journal of Optics* 17, 8, 085101 (2015).

# Flexible multilayer oxide based device

## 3.1 Flexible Visible Blind Imaging Device enabled by Oxygen Deficient Zinc Oxide Sensing Elements

The work related to this Chapter has been peer-reviewed and published in *Advanced Electronic Materials*.

The full paper can be obtained via http://dx.doi.org/10.1002/aelm.201500264

This work can be cited as: **P. Gutruf**, S.Walia, M. Bhaskaran and S. Sriram "Flexible visible blind imaging device enabled by oxygen deficient zinc oxide sensing elements" in press *Advanced Electronic Materials* (2015) DOI: 10.1002/aelm.201500264

# Incorporation of high temperature processed oxides for stretchable electronics

## 4.1 Transparent Functional Oxide Stretchable Electronics: Micro-Tectonics Enabled High Strain Electrodes

The work related to this Chapter has been peer-reviewed and published in *NPG Asia Materials*.

The full paper can be obtained via http://dx.doi.org/ 10.1038/am.2013.41

This work can be cited as: **P Gutruf**, C M Shah, S Walia, H Nili, A S Zoolfakar, C Karnutsch, K Kalantar-zadeh, S Sriram, M Bhaskaran "Transparent functional oxide stretchable electronics: Micro-tectonics enabled high strain electrodes" *NPG Asia Materials*, 5, 9, e62 (2013).

# Stretchable zinc oxide based devices

## 5.1 Stretchable and Tunable Microtectonic ZnO-Based Sensors and Photonics.

The work related to this Chapter has been peer-reviewed and published in *Small*.

The full paper can be obtained via http://dx.doi.org/10.1002/smll.201500729

This work can be cited as: **P Gutruf**, E Zeller, S Walia, H Nili, S Sriram, and M Bhaskaran. "Stretchable and Tunable Microtectonic ZnO-Based Sensors and Photonics." *Small, 11, 35,* 906-912 (2015).

# Stretchable Photonics: Gratings and Resonant Structures

## 6.1 Mechanically Tunable High Refractive Index Contrast $TiO_2$–PDMS Gratings

The work related to this Chapter has been peer-reviewed and published in *Advanced Optical Materials*.

The full paper can be obtained via http://dx.doi.org/10.1002/adom.201500346

This work can be cited as: **P Gutruf,** E Zeller, S Walia, S Sriram and M Bhaskaran "Mechanically Tunable High Refractive Index Contrast $TiO_2$–PDMS Gratings" *Advanced Optical Materials,* 3, 11, 1565-1569 (2015).

## 6.2 Mechanically Tunable Dielectric Resonator Metasurfaces at Visible Frequencies

The work related to this Chapter has been peer-reviewed and published in *ACS Nano*.

The full paper can be obtained via http://dx.doi.org/10.1021/acsnano.5b05954

This work can be cited as: **P Gutruf,** C Zou, W Withayachumnankul, M Bhaskaran, S Sriram and C Fumeaux "Mechanically Tunable Dielectric Resonator Antennas at Visible Frequencies" *ACS Nano,* Article ASAP (2015) DOI: 10.1021/acsnano.5b05954

# Conclusion and Future Work

## 7.1 Conclusion

In conclusion this thesis explores new avenues to integrate functional materials with a focus on metal oxides into flexible and stretchable platforms. Scientific insight towards the behaviour of thin films on flexible and stretchable platforms is presented and strategies to reduce the strain sensitivity are explored. Furthermore the interplay of metal films and metal oxides, namely zinc oxide is investigated in the context of the first demonstration of a visible blind UV imaging device. Additionally and significantly, a novel method of engineering full stretchability of brittle oxides on elastomeric materials is shown. The responsible effect which is named micro-tectonics is explored in detail and a model for electrical conduction under strain is established. The effect is used to create micro-tectonic gas and UV sensors that allow for elevated sensitivity as well as stretchability, outperforming its rigid counterparts. The novel fabrication method which was developed for the micro-tectonic device is also exploited to integrate high resolution patterned dielectrics into elastomeric materials to create tunable optics. Diffractive optics such as tunable gratings are shown and analysed in detail. The devices exhibit excellent linear tunability alongside with an accurate representation of local strain. Additionally the size of the dielectrics in an elastomeric matrix could be reduced to sub wavelength size allowing for the first demonstration of tunable dielectric resonators at visible frequencies allowing a study in the coupling behaviour of such devices.

## 7.2 Outlook

The methods and scientific insight presented in this thesis form a solid base for future projects. The insights gained in chapter 2.1 allows for the creation of devices with strain sensitivity engineering, while this study was performed with the prevalent material combination of gold and polyimide, future studies with material combinations can gather new insight. Material combinations such as PET and gold or oxides such as ITO and PET would gather substantial insight with regard to strain sensitivity of well adhered thin films on flexible materials.

The insights gained in chapter 2.2 allow for a multifaceted approach to terahertz metamaterials, the fabrication method presented in this chapter is an evolution of the method used in 2.1. Through the excellent hard contact to a lithography mask by the vertically protruding polyimide layer a feature size of down to one micro meter are easily achievable with photolithography using a UV exposure source. Furthermore the isolation layer used in the work, namely SU-8, is available from a thickness of 500 nm up to 75µm. This allows for immense design freedom and therefore many thinkable designs of multilayer terahertz metamaterials, especially designs requiring a high resolution capability.

The flexible visible-blind UV imaging array presented in chapter 3.1 which is enabled through the insights gained in chapter 2.1 and 2.2 exhibits the forefront of flexible technology . The device show cases the advantages of flexible imaging devices, namely cost effective large area capability, which is crucial for a low noise imaging device. Future works can include flexible active components for higher pixel counts to reduce crosstalk which is common problem in resistive based sensing or memory arrays. The complexity shown by the system is also a motivation alongside other integrated flexible devices demonstrating the capability of flexible electronic technology.

The introduction of micro-tectonics which enable an entirely stretchable devices without the use of rigid island approaches or pre strained substrates as demonstrated in chapter 4.1 and 5.1. Furthermore these devices exhibit a very strong robustness enabled by the strong adhesion of PDMS and the micro-tectonic oxide. The ubiquitous synthesis route also allows for the introduction of various oxide or semiconductor materials which enables a variety of novel devices. The stretchability also allows for a design as a wearable device due to the stretchability of micro-tectonic devices (15%), which is generally the range of strain observed on skin on most body parts.

Dielectric grating devices as presented in chapter 6.1 are naturally superior to its organic counterparts by harnessing the high refractive index contrast offered by elastomer and dielectric material. This makes these device very efficient and enable ultra-thin architectures, alongside with the highly linear tunability shown in the work they offer opportunities towards real world applications such as tunable filters, strain sensors and beam steering. Furthermore such gratings can be used to couple to polymer optics which is generally considered a challenge.

Dielectric resonant photonic devices offer a distinct advantage over metal based device at visible frequencies by reducing ohmic losses significantly, by embedding such devices into an elastomeric platform a tunable resonator design is demonstrated in chapter 6.2. While creating a fundamental insight into the coupling behaviour of such resonant devices, they also offer the opportunity for light weight adaptable designs enabling a novel class of optics. Furthermore fundamental building blocks of such lightweight tunable optics such as absorbers, plasmonic launchers are thinkable.

# References


[1] T. Sekitani, T. Someya, *Advanced Materials* **2010**, *22*, 2228-46

[2] T. Sekitani, H. Nakajima, H. Maeda, T. Fukushima, T. Aida, K. Hata, T. Someya, *Nature materials* **2009**, *8*, 494-9

[3] D. J. Lipomi, B. C. K. Tee, M. Vosgueritchian, Z. Bao, *Advanced Materials* **2011**, *23*, 1771-5

[4] T. Someya, T. Sekitani, S. Iba, Y. Kato, H. Kawaguchi, T. Sakurai, *Proceedings of the National Academy of Sciences of the United States of America* **2004**, *101*, 9966-70

[5] T. Sekitani, T. Yokota, U. Zschieschang, H. Klauk, S. Bauer, K. Takeuchi, M. Takamiya, T. Sakurai, T. Someya, *Science* **2009**, *326*, 1516-9

[6] T. Sekitani, U. Zschieschang, H. Klauk, T. Someya, *Nature Materials* **2010**, *9*, 1015-22

[7] A. Chortos, G. I. Koleilat, R. Pfattner, D. Kong, P. Lin, R. Nur, T. Lei, H. Wang, N. Liu, Y. C. Lai, *Advanced Materials* **2015**,

[8] B. C. Tee, C. Wang, R. Allen, Z. Bao, *Nature nanotechnology* **2012**, *7*, 825-32

[9] Z. Bao, A. J. Lovinger, J. Brown, *Journal of the American Chemical Society* **1998**, *120*, 207-8

[10] J. He, R. G. Nuzzo, J. Rogers, *Proceedings of the IEEE* **2015**, *103*, 619-32

[11] F. Xu, Y. Zhu, *Advanced Materials* **2012**, *24*, 5117-22

[12] S. Yao, Y. Zhu, *Nanoscale* **2014**, *6*, 2345-52

[13] Y. Qi, J. Kim, T. D. Nguyen, B. Lisko, P. K. Purohit, M. C. McAlpine, *Nano letters* **2011**, *11*, 1331-6

[14] J. Yi, J. M. Lee, W. I. Park, *Sensors and Actuators B: Chemical* **2011**, *155*, 264-9

[15] T. Rai, P. Dantes, B. Bahreyni, W. S. Kim, *Electron Device Letters, IEEE* **2013**, *34*, 544-6

[16] D. Kim, G. Shin, J. Yoon, D. Jang, S.-J. Lee, G. Zi, J. S. Ha, *Nanotechnology* **2013**, *24*, 315502

[17] M. Park, J. Im, M. Shin, Y. Min, J. Park, H. Cho, S. Park, M.-B. Shim, S. Jeon, D.-Y. Chung, *Nature nanotechnology* **2012**, *7*, 803-9

[18] M. G. Chung, D.-H. Kim, D. K. Seo, T. Kim, H. U. Im, H. M. Lee, J.-B. Yoo, S.-H. Hong, T. J. Kang, Y. H. Kim, *Sensors and Actuators B: Chemical* **2012**, *169*, 387-92

[19] L. Yuan, X.-H. Lu, X. Xiao, T. Zhai, J. Dai, F. Zhang, B. Hu, X. Wang, L. Gong, J. Chen, *Acs Nano* **2011**, *6*, 656-61

[20] M. Segev-Bar, A. Landman, M. Nir-Shapira, G. Shuster, H. Haick, *ACS applied materials & interfaces* **2013**, *5*, 5531-41

[21] K.-Y. Chun, Y. Oh, J. Rho, J.-H. Ahn, Y.-J. Kim, H. R. Choi, S. Baik, *Nature nanotechnology* **2010**, *5*, 853-7

[22] S. P. Lacour, S. Wagner, Z. Huang, Z. Suo, *Applied physics letters* **2003**, *82*, 2404-6

[23] S. P. Lacour, J. Jones, S. Wagner, T. Li, Z. Suo, *Proceedings of the IEEE* **2005**, *93*, 1459-67

[24] S. P. Lacour, J. Jones, Z. Suo, S. Wagner, *Electron Device Letters, IEEE* **2004**, *25*, 179-81

[25] S. P. Lacour, D. Chan, S. Wagner, T. Li, Z. Suo, *Applied Physics Letters* **2006**, *88*, 204103

[26] T. Adrega, S. Lacour, *Journal of Micromechanics and Microengineering* **2010**, *20*, 055025

[27] N. Lu, X. Wang, Z. Suo, J. Vlassak, *Applied Physics Letters* **2007**, *91*, 221909

[28] D.-Y. Khang, J. A. Rogers, H. H. Lee, *Adv. Funct. Mater* **2009**, *19*, 1526-36

[29] N. Bowden, S. Brittain, A. G. Evans, J. W. Hutchinson, G. M. Whitesides, *Nature* **1998**, *393*, 146-9

[30] S. Kim, H. Y. Jeong, S. K. Kim, S.-Y. Choi, K. J. Lee, *Nano letters* **2011**, *11*, 5438-42

[31] J. Kim, A. Banks, H. Cheng, Z. Xie, S. Xu, K. I. Jang, J. W. Lee, Z. Liu, P. Gutruf, X. Huang, *Small* **2015**, *11*, 906-12

[32] Y. Zhang, H. Fu, Y. Su, S. Xu, H. Cheng, J. A. Fan, K.-C. Hwang, J. A. Rogers, Y. Huang, *Acta Materialia* **2013**, *61*, 7816-27

[33] Y. Zhang, S. Wang, X. Li, J. A. Fan, S. Xu, Y. M. Song, K. J. Choi, W. H. Yeo, W. Lee, S. N. Nazaar, *Advanced Functional Materials* **2014**, *24*, 2028-37

[34] S. Xu, Y. Zhang, J. Cho, J. Lee, X. Huang, L. Jia, J. A. Fan, Y. Su, J. Su, H. Zhang, *Nature communications* **2013**, *4*, 1543

[35] G. A. Salvatore, N. Münzenrieder, T. Kinkeldei, L. Petti, C. Zysset, I. Strebel, L. Büthe, G. Tröster, *Nature communications* **2014**, *5*,

[36] Y. Sun, J. A. Rogers, *ADVANCED MATERIALS-DEERFIELD BEACH THEN WEINHEIM-* **2007**, *19*, 1897

[37] D.-H. Kim, R. Ghaffari, N. Lu, J. A. Rogers, *Annual review of biomedical engineering* **2012**, *14*, 113-28

[38] M. A. Meitl, Z.-T. Zhu, V. Kumar, K. J. Lee, X. Feng, Y. Y. Huang, I. Adesida, R. G. Nuzzo, J. A. Rogers, *Nature Materials* **2006**, *5*, 33-8

[39] C. Dagdeviren, B. D. Yang, Y. Su, P. L. Tran, P. Joe, E. Anderson, J. Xia, V. Doraiswamy, B. Dehdashti, X. Feng, *Proceedings of the National Academy of Sciences* **2014**, *111*, 1927-32

[40] T.-i. Kim, J. G. McCall, Y. H. Jung, X. Huang, E. R. Siuda, Y. Li, J. Song, Y. M. Song, H. A. Pao, R.-H. Kim, *Science* **2013**, *340*, 211-6

[41] J. Viventi, D.-H. Kim, L. Vigeland, E. S. Frechette, J. A. Blanco, Y.-S. Kim, A. E. Avrin, V. R. Tiruvadi, S.-W. Hwang, A. C. Vanleer, *Nature neuroscience* **2011**, *14*, 1599-605

[42] D. Karnaushenko, B. Ibarlucea, S. Lee, G. Lin, L. Baraban, S. Pregl, M. Melzer, D. Makarov, W. M. Weber, T. Mikolajick, *Advanced healthcare materials* **2015**,

[43] D. D. Karnaushenko, D. Karnaushenko, D. Makarov, O. G. Schmidt, *NPG ASIA MATERIALS* **2015**, *7*,

[44] H. Tao, A. Strikwerda, K. Fan, C. Bingham, W. Padilla, X. Zhang, R. Averitt, *arXiv preprint arXiv:0808.0454* **2008**,

[45] M. Melzer, M. Kaltenbrunner, D. Makarov, D. Karnaushenko, D. Karnaushenko, T. Sekitani, T. Someya, O. G. Schmidt, *Nature communications* **2015**, *6*,

[46] K. Nomura, H. Ohta, A. Takagi, T. Kamiya, M. Hirano, H. Hosono, *Nature* **2004**, *432*, 488-92

[47] M. Kaltenbrunner, M. S. White, E. D. Głowacki, T. Sekitani, T. Someya, N. S. Sariciftci, S. Bauer, *Nature communications* **2012**, *3*, 770

[48] S. Xu, Y. Qin, C. Xu, Y. Wei, R. Yang, Z. L. Wang, *Nature nanotechnology* **2010**, *5*, 366-73

[49] J. Zhou, Y. Gu, P. Fei, W. Mai, Y. Gao, R. Yang, G. Bao, Z. L. Wang, *Nano letters* **2008**, *8*, 3035-40

[50] R. Yu, L. Dong, C. Pan, S. Niu, H. Liu, W. Liu, S. Chua, D. Chi, Z. L. Wang, *Advanced Materials* **2012**, *24*, 3532-7

[51] R.-H. Kim, D.-H. Kim, J. Xiao, B. H. Kim, S.-I. Park, B. Panilaitis, R. Ghaffari, J. Yao, M. Li, Z. Liu, *Nature materials* **2010**, *9*, 929-37

[52] L. Xu, S. R. Gutbrod, Y. Ma, A. Petrossians, Y. Liu, R. C. Webb, J. A. Fan, Z. Yang, R. Xu, J. J. Whalen, *Advanced Materials* **2015**, *27*, 1731-7

[53] H. J. Chung, M. S. Sulkin, J. S. Kim, C. Goudeseune, H. Y. Chao, J. W. Song, S. Y. Yang, Y. Y. Hsu, R. Ghaffari, I. R. Efimov, *Advanced healthcare materials* **2014**, *3*, 59-68

[54] J. Kim, A. Banks, Z. Xie, S. Y. Heo, P. Gutruf, J. W. Lee, S. Xu, K. I. Jang, F. Liu, G. Brown, *Advanced Functional Materials* **2015**, *25*, 4761-7

[55] W. H. Yeo, Y. S. Kim, J. Lee, A. Ameen, L. Shi, M. Li, S. Wang, R. Ma, S. H. Jin, Z. Kang, *Advanced Materials* **2013**, *25*, 2773-8

[56] C. Dagdeviren, Y. Shi, P. Joe, R. Ghaffari, G. Balooch, K. Usgaonkar, O. Gur, P. L. Tran, J. R. Crosby, M. Meyer, *Nature materials* **2015**,

[57] D. Marculescu, R. Marculescu, N. H. Zamora, P. S. Marbell, P. K. Khosla, S. Park, S. Jayaraman, S. Jung, C. Lauterbach, W. Weber, *Proceedings of the IEEE* **2003**, *91*, 1995-2018

[58] C. H. Lee, Y. Ma, K. I. Jang, A. Banks, T. Pan, X. Feng, J. S. Kim, D. Kang, M. S. Raj, B. L. McGrane, *Advanced Functional Materials* **2015**,

# Appendix

## 7.3 Supplementary Information for Chapter 2.1

# Supplementary Information:

# Strain response of stretchable micro-electrodes: Controlling sensitivity with serpentine designs and encapsulation

Philipp Gutruf, Sumeet Walia, Md Nur Ali, Sharath Sriram,[a)] and Madhu Bhaskaran[a)]

Functional Materials and Microsystems Research Group, School of Electrical and Computer Engineering, RMIT University, GPO Box 2476, Melbourne, Victoria, Australia.

[a)]Authors to whom correspondence should be addressed. Electronic mail: sharath.sriram@gmail.com, madhu.bhaskaran@gmail.com

**Electron Microscopy Analysis**

In order to confirm the occurrence of micro-cracking, electron microscopy was performed using a field emission scanning electron microscope. Results for the straight gold electrodes before and after dynamic resistance measurements (Fig. S1). It is apparent that micro-cracks appear after the resistance measurements. Furthermore, the surface of the serpentine electrodes was imaged after the testing. In these cases, the micro-cracking effect of the dynamic resistance measurements on the gold layer reduces with a higher angle of curvature (Fig. S2).

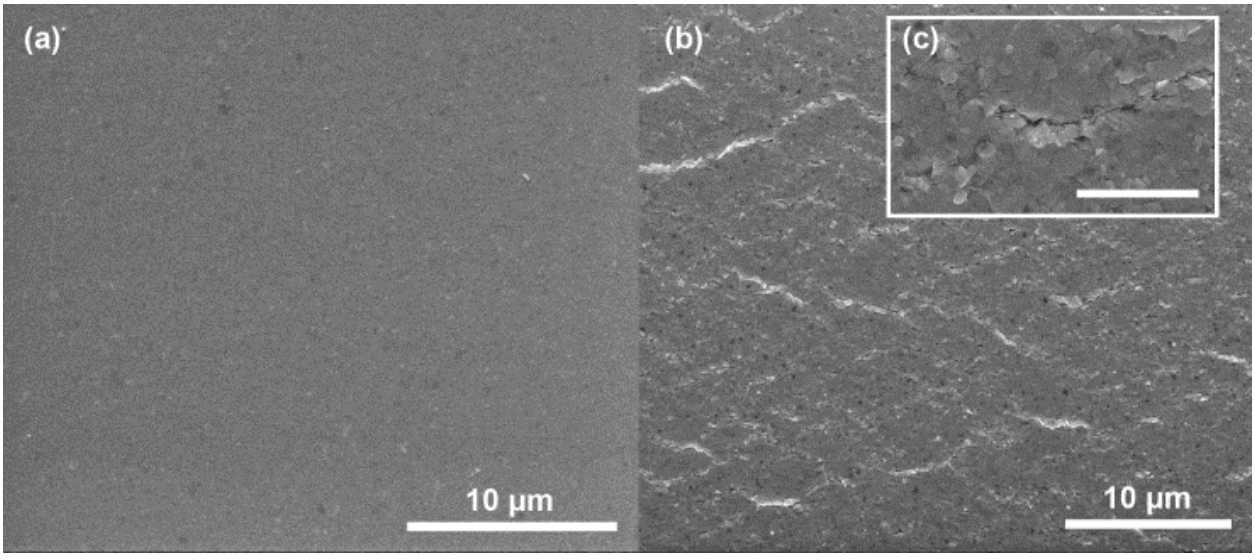


FIG. S1. Straight gold electrodes (a) before dynamic measurements and (b) after dynamic measurements. The stretched electrodes in (b) have visible micro-cracks, shown at greater magnification in the inset (c) where the scale bar is 2 µm.

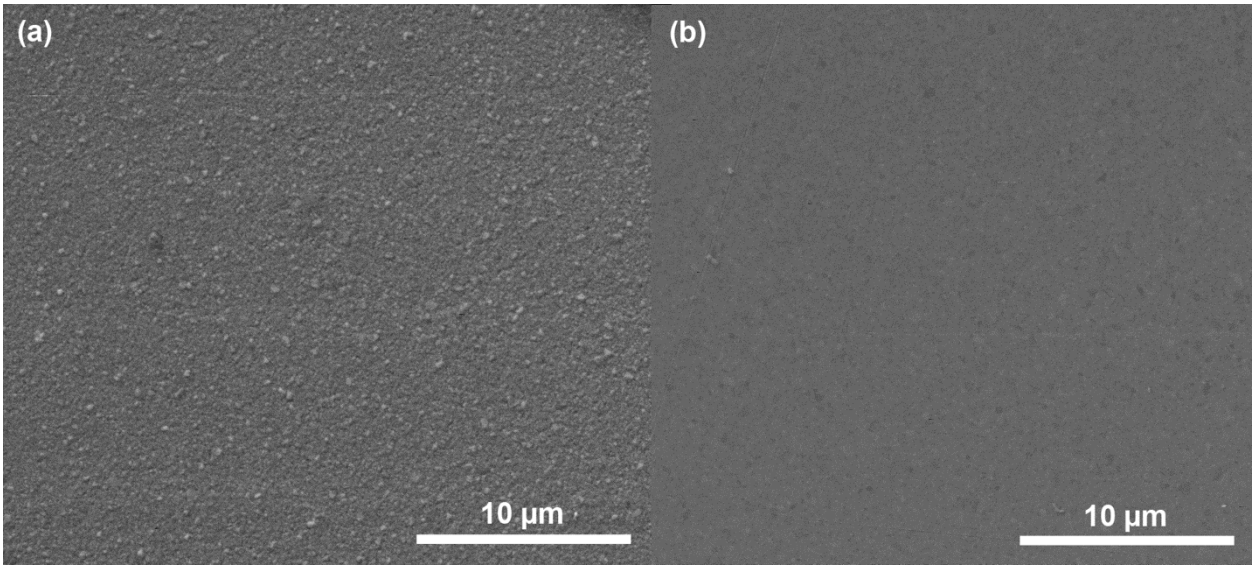


FIG. S2. Electron micrographs of gold electrodes after dynamic measurements: (a) 60° electrodes with roughened surface [no apparent micro-cracking as in Fig. S1(b,c)] and (b) 90° electrodes showing smooth topography with no induced micro-cracking.

## 7.4 Supplementary Information for Chapter 3.1

# Supporting Information

for *Adv. Electron. Mater.,* DOI: 10.1002/aelm.201500264

# Visible-Blind UV Imaging with Oxygen-Deficient Zinc Oxide Flexible Devices

*Philipp Gutruf,* Sumeet Walia, Sharath Sriram, and Madhu Bhaskaran**

## Supporting Information

for
DOI: 10.1002/aelm.201500264

# Visible-blind UV imaging with oxygen-deficient zinc oxide flexible devices

*Philipp Gutruf,* Sumeet Walia, Sharath Sriram, and Madhu Bhaskaran**

[*] Functional Materials and Microsystems Research Group and Micro Nano Research Facility, RMIT University, Melbourne, Victoria 3000 (Australia)
E-mail: philippgutruf@googlemail.com, madhu.bhaskaran@gmail.com

Keywords: flexible electronics, ZnO, UV sensing, visible-blind imaging, oxygen deficiency

### Thin Film Analysis

*X-ray photoelectron spectroscopy analysis*

In order to compare the difference in oxygen deficiency of a stoichiometric *vs.* an oxygen deficient film, we conducted an XPS scan on the films used in this study and compared it with a stoichiometric zinc oxide film. It is evident that in the case of films used in this study, an oxygen deficiency is maintained throughout the depth of the film, while the stoichiometric film shows a slight oxygen deficiency only at the surface and retains its as-deposited stoichiometry through the bulk of the film.

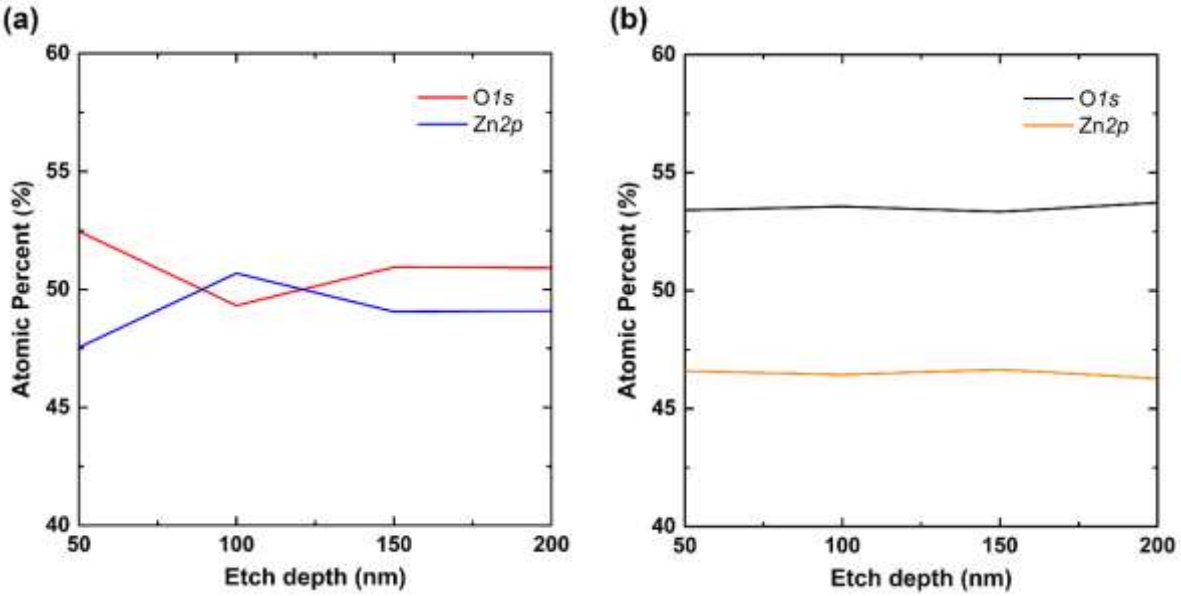


**Figure S1**. Comparison of atomic percentage of Zn and O in: (a) stoichiometric and (b) oxygen-deficient thin films of ZnO.

*X-ray diffraction analysis*

In order to characterise the zinc oxide (ZnO) thin film sensing elements and gain insight into the crystalline structure, we performed X-ray diffraction analysis. In the result plotted in **Figure S2**, a clear ZnO (002) peak can be observed confirming the crystalline nature of the thin film.

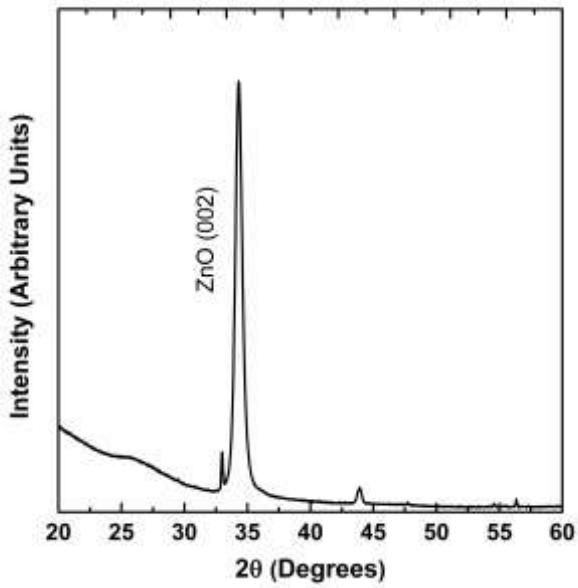


**Figure S2.** X-ray diffraction analysis of the sputtered zinc oxide films on polyimide showing preferential crystalline orientation.

*Transmission analysis*

In order to estimate the spectral sensitivity of the sensing pixels, we performed transmission measurement of ZnO thin films deposited onto amorphous glass slides. The films were deposited with identical parameters to the films used in the imaging arrays. The result shown in **Figure S3** shows clear absorption from 280 nm to 400 nm indicating spectral sensitivity of ZnO in this range.

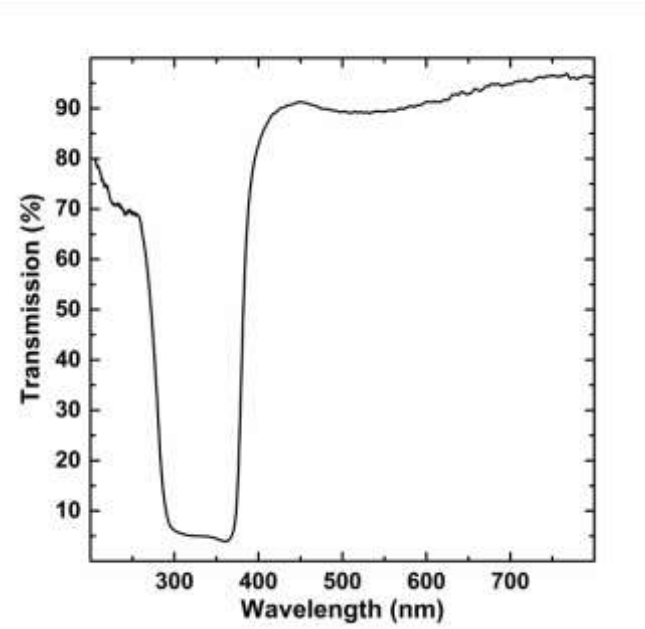


**Figure S3.** Transmission measurement showing high absorption of the ZnO thin films in the spectral range of 280 nm to 400 nm.

*Spectral sensitivity*

In order to verify the spectral sensitivity, which was estimated from the transmission measurement, we irradiated a single pixel with multiple wavelengths to test its response. For the test we used a Thorlabs LED4D007 light source with 4 LED light sources (365 nm, 85 mW; 455 nm, 310 mW; 530 nm, 100 mW; 625 nm, 240 mW). In **Figure S4** a strong response to 365 nm can be observed. The response to the 455 nm can be attributed to the wide spectrum emitted by the deep blue LED (400-500 nm), which falls within the spectral

sensitivity of the ZnO pixel. The visible colour light sources show negligible response, as expected.

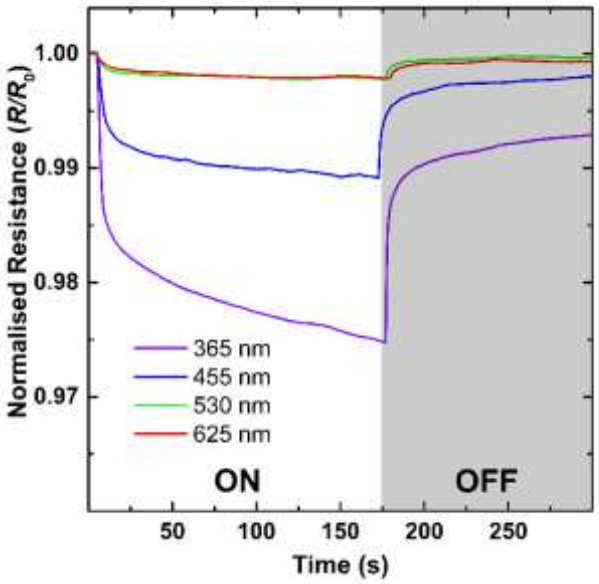


**Figure S4.** Pixel response to light sources of different wavelengths.

*Pixel current–voltage characteristics*

To determine the nature of the Cu/ZnO interface, current–voltage (*I–V*) characteristics without and with UV illumination were acquired (**Figure S5**) under, a bias sweep from -10 V to 10V. The analysis was performed with and without UV illumination. The *I–V* analysis confirms the ohmic nature of the Cu/ZnO interface. This allows for a free choice in measurement bias.

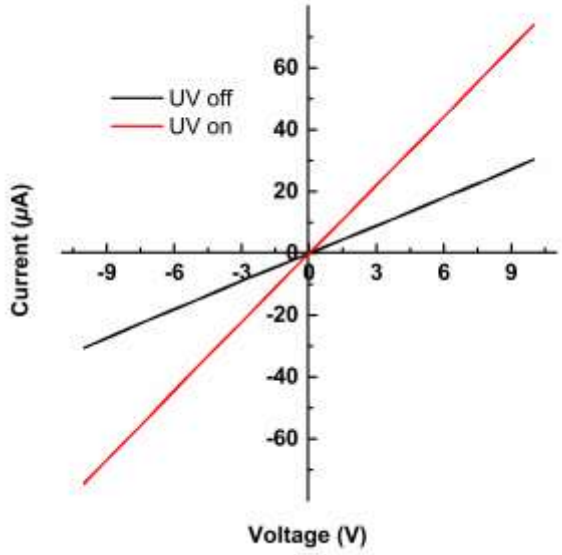


**Figure S5.** *I–V* characteristics of a single pixel in its initial state (UV off) and under UV illumination (UV on with 26.6 mW/cm$^2$ illumination).

**Imaging Arrays with Convex Curvature**

In order to complete the mechanical evaluation of the imaging array, we recorded images by bending the array in a convex shape. Images were recorded under conditions identical to those used for the flat (Figure 4) and concave curvature (Figure 5) arrays. The bending radius of 5 cm was achieved by affixing the sensor to a PVC tube. The results obtained are presented in **Figure S6**. It can be seen in Figure S5b that the high intensity, low area exposure has an asymmetric shape compared to the flat sensor. This is expected due to the curvature of the array. A similar phenomenon can be observed in the line exposure (Figure S6c), where curvature of the array causes the outer sensing elements to receive little UV radiation, due to the absence of direct optical path to the UV source. The same can be observed for the cross-shaped exposure.

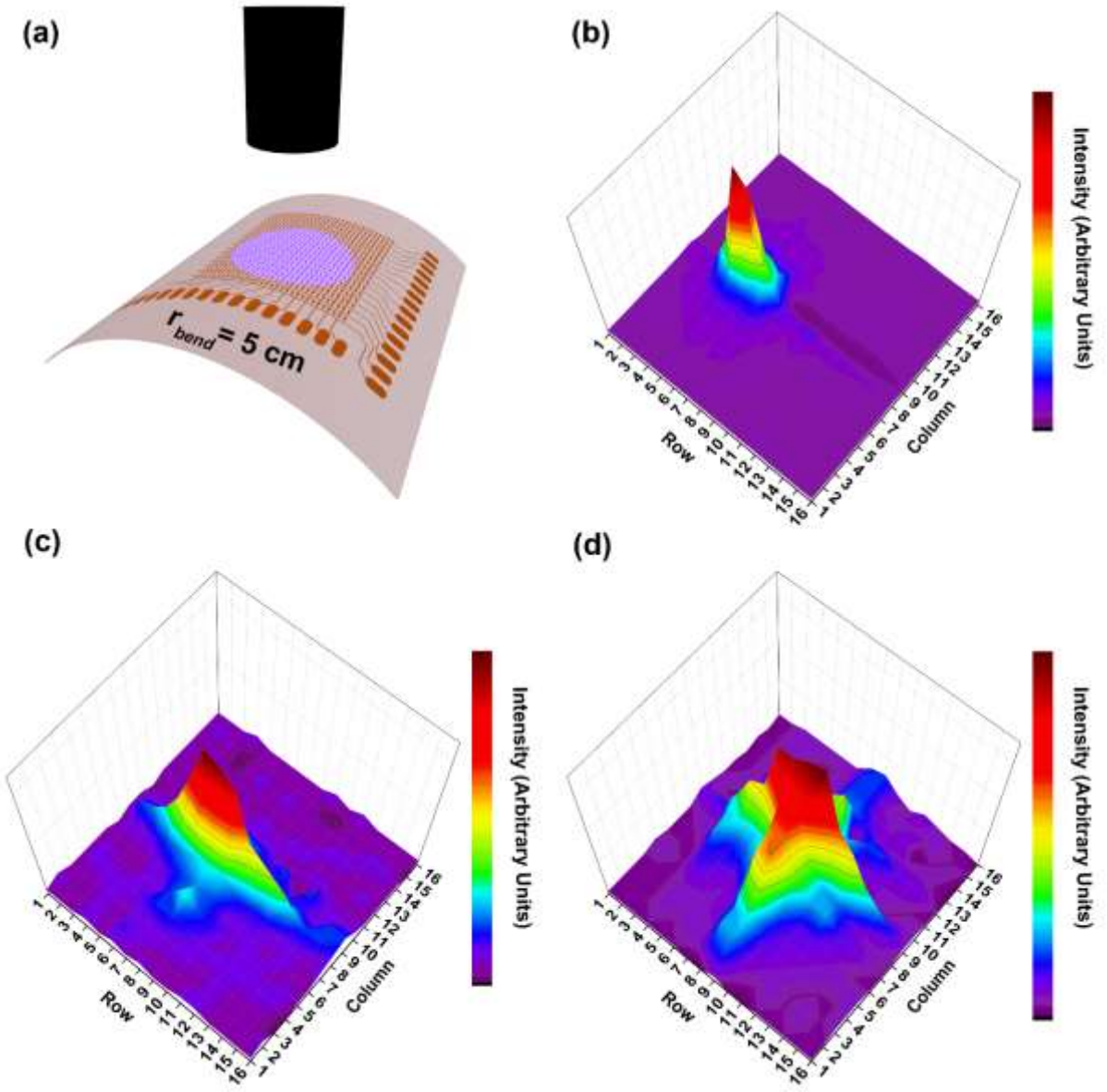


**Figure S6.** (a) Schematic of the test setup with perpendicularly-mounted UV source (365 nm), with an imaging array with convex curvature (bending radius $r_{bend}$ of 5 cm). Three-dimensional representation of imaging results are presented for high intensity exposure (25 mW/cm$^2$) over a small area in (b) and for medium intensity (10 mW/cm$^2$) exposure through masks, with a single line exposure in (c) and a cross-shaped exposure in (d).

**Device Failure Analysis *via in situ* Electron Microscopy**

In the main manuscript, we demonstrate the bendability and function of the device under convex and concave bending states. During testing no failure was observed. For the ultimate device failure analysis, we used the brittle ZnO thin films on polyimide, in the configuration used in the device.[S1] In order to determine the failure mechanism, we employed *in situ* electron microscopy where strain is applied to the ZnO coated polyimide. The result is displayed in **Figure S7** where we can observe no alterations in the film morphology up to a strain of 2%. Under a strain of 4% (which is also the elastic limit of polyimide), we observe the onset of micro-cracking which still does not result in the failure of the film but only in a temporary increase of resistance.[S2] Subsequent increase in strain, deforms the device permanently due to plastic deformation in the polyimide which results in a marginal increase in micro-cracking. However, no delamination of the film is observed.

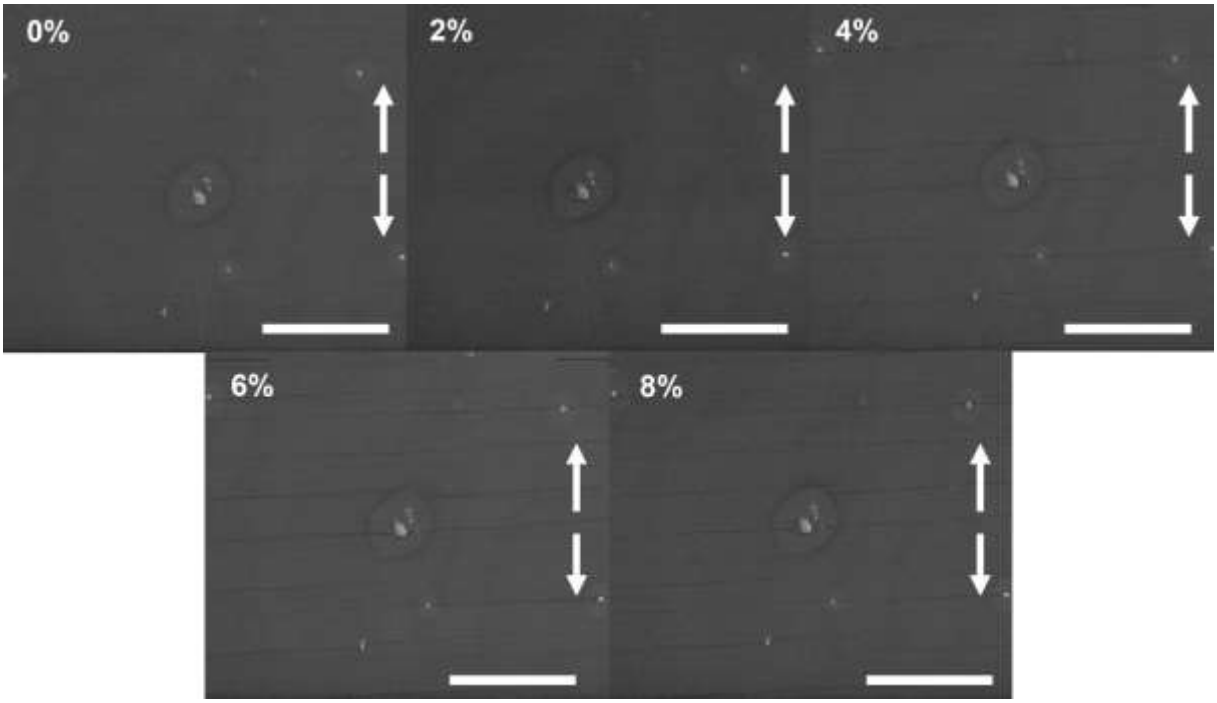


**Figure S7.** *In situ* electron microscopy analysis of the ZnO film on Polyimide with increasing strain. The scale bars in the figure represent 20 μm with the applied strain displayed in the top left corner. The direction of strain is indicated by arrows.

**Control and Evaluation Electronics**

In order to read out the imaging array, a National instruments (NI) cDAQ-9174 system with a NI 9205 32-channel analog voltage input module was used. The signal was read out of each row in differential mode. The differential mode allows for a common mode noise suppression, and therefore, boosts signal-to-noise ratios allowing for a better imaging performance. For the channel selection, a NI 9264 16-Channel analog output was used. This allows for a flexible gain of the system which can be tailored to the application. In this work, it is fixed to 10 V to achieve a high sensitivity. The resistive elements are connected according to the schematic shown in **Figure S8**. The resistors in each row are in series with an individual reference resistor, forming a voltage divider, which is shared for each column in the array. The reference resistor is connected to a multiplexer (MUX) which allows for a differential voltage measurement across each reference resistor in a sequential manner. The differential measurement, if not active is switched to high impedance. In practice the measurement is carried out in the following manner: Row 1 is biased by the row selector. Now the sequential read out of the column starts with $R_{ref\_1}$ through to $R_{ref\_16}$. Subsequently all 16 rows are selected and the column read out to is carried out to read in all elements of the array. The signal gathered from each element is saved in an array and digitally compared against a prior recorded dark reference to compile the image.

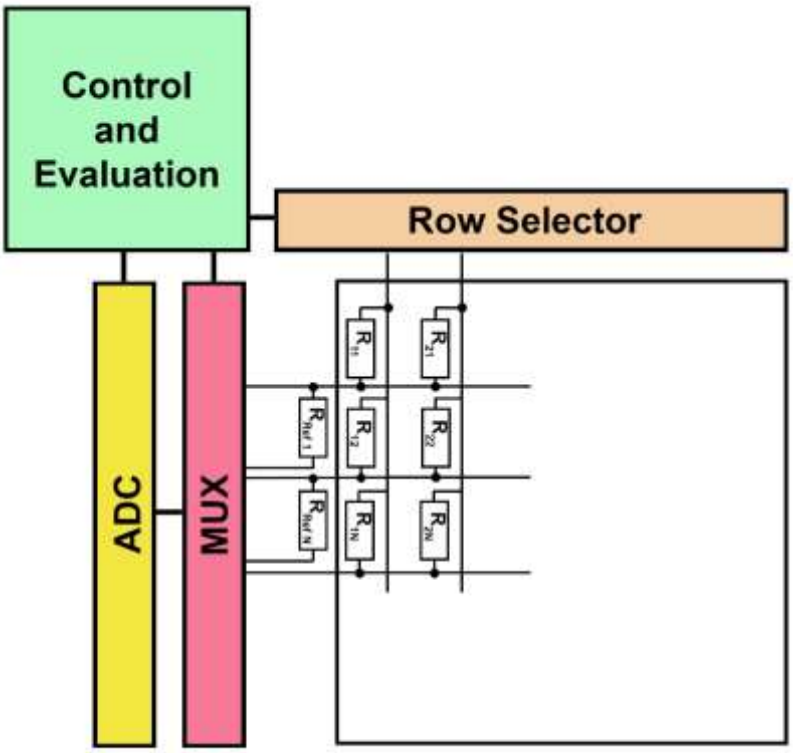


**Figure S8.** Block diagram representation of the internal electrical connection of the single pixels and their connection to peripheral elements.

## References

[S1] N. Lu, X. Wang, Z. Suo, J. Vlassak, *Applied Physics Letters* **2007**, *91*, 221909.

[S2] P. Gutruf, S. Walia, M. N. Ali, S. Sriram, M. Bhaskaran, *Applied Physics Letters* **2014**, *104*, 021908.

## 7.5 Supplementary Information for Chapter 4.1

# Supplementary Information:

# Transparent functional oxide stretchable electronics:

# Micro-tectonics enabled high strain electrodes

Philipp Gutruf[1,2], Charan Manish Shah[1], Sumeet Walia[1], Hussein Nili[1], Ahmad Sabirin Zoolfakar[1], Christian Karnutsch[2], Kourosh Kalantar-zadeh,[1] Sharath Sriram[1,*] & Madhu Bhaskaran[1,*]

[1] Functional Materials and Microsystems Research Group, School of Electrical and Computer Engineering, RMIT University, Melbourne, Victoria, Australia.

[2] Institute for Optofluidics and Integrated Nanophotonics, Department of Electrical Engineering & Information Technology, Karlsruhe University of Applied Sciences, Karlsruhe, Germany.

* Correspondence and requests for materials should be addressed to S.S. (sharath.sriram@rmit.edu.au) and M.B. (madhu.bhaskaran@rmit.edu.au).

**Energy dispersive X-ray analysis**

To demonstrate that no platinum was diffused in the functional oxide layers, energy dispersive X-ray analysis was performed for both ITO and ZnO thin films on PDMS. These results are presented in Figs. S1 and S2. The results demonstrate the high purity of the materials used. Specific to the PDMS substrate is the strong Si peak combined with a small O peak which can be observed in both the results. Figure S1 shows a strong In and Sn peak as anticipated, with no Pt peak present. Figure S2 shows a similar result. Strong O and Zn peaks are detected with no traces of Pt.

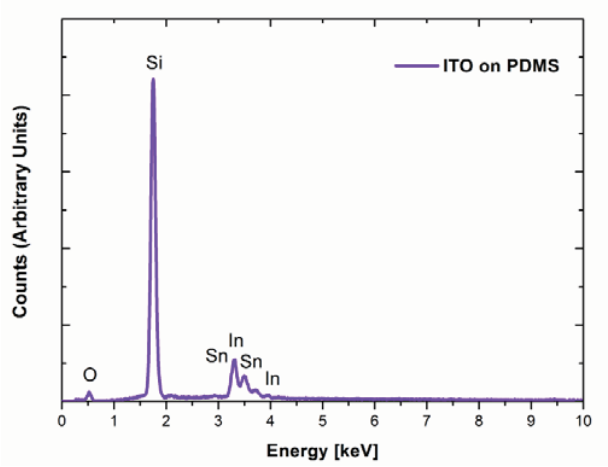


**Figure S1** EDX analysis of an ITO on PDMS structure following transfer and Pt removal. The analysis was performed in low vacuum mode at 30 kV accelerating voltage.

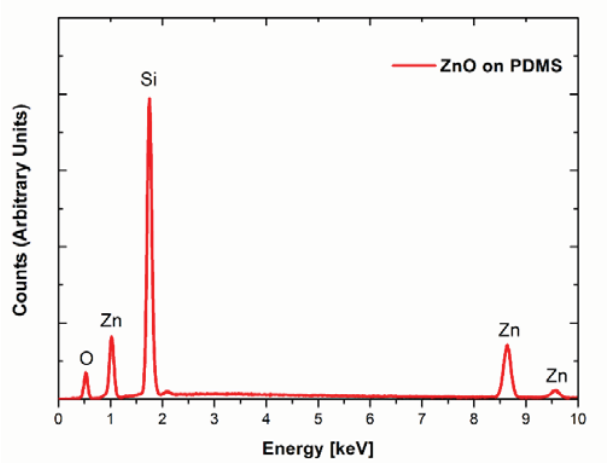


**Figure S2** EDX analysis of a ZnO on PDMS structure following transfer and Pt removal. The analysis was performed in low vacuum mode at 30 kV accelerating voltage.

**Conductive atomic force microscopy**

To support the resolution experiments, we performed a conductive atomic force microscopy (AFM) imaging. The result presented in Fig. S3 shows a gap of 5 µm with the PDMS incorporating the ITO plates. The height difference in the layers is due to the absence of the platinum transfer layer as well as thermal stress being applied during the curing step. The PDMS buckles up in the absence of the brittle and not deformable ITO. Furthermore, Fig. S3 shows the high contrast between the conductive ITO and the insulating PDMS.

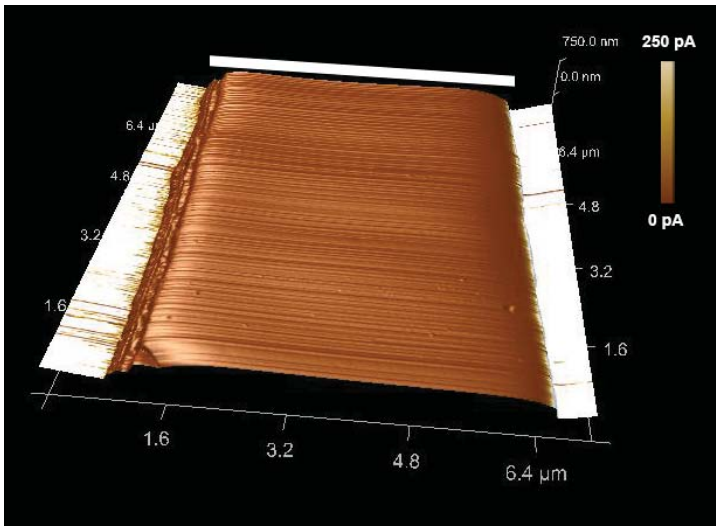


**Figure S3** Atomic force microscopy conductivity mapping of a patterned 5 µm gap in the ITO layer. The scale bar represents 5 µm.

## 7.6 Supplementary Information for Chapter 5.1

NANO MICRO small

# Supporting Information

for *Small.,* DOI: 10.1002/smll.201500729

## Stretchable and Tunable Microtectonic ZnO-Based Sensors and Photonics

*Philipp Gutruf, Eike Zeller, Sumeet Walia, Hussein Nili, Sharath Sriram,* and Madhu Bhaskaran**

# SUPPORTING INFORMATION
# for

DOI: 10.1002/smll.201500729
**Article type:** Full Paper

**Stretchable and tunable micro-tectonic ZnO-based sensors and photonics**

*By Philipp Gutruf, Eike Zeller, Sumeet Walia, Hussein Nili, Sharath Sriram,* and Madhu Bhaskaran**

[*] Mr. Philipp Gutruf, Dr. Eike Zeller, Dr. Sumeet Walia, Dr. Hussein Nili, Dr. Sharath Sriram, Dr. Madhu Bhaskaran
Functional Materials and Microsystems Research Group and Micro Nano Research Facility, RMIT University, Melbourne, Victoria (Australia)
E-mail: sharath.sriram@rmit.edu.au, madhu.bhaskaran@rmit.edu.au

Keywords: stretchable electronics, ZnO, gas sensing, UV sensing, stretchable gratings

**Performance comparison of a rigid and micro-tectonic gas sensor**

**Figure S1** shows the dynamic response of a ZnO/PDMS and ZnO/silicon sensor under cyclic exposure to hydrogen (200 sccm of 1% hydrogen balanced in zero air) for 10 min followed by 35 min recovery in zero air cycles. The sensors were kept at a constant temperature of 100 °C throughout the measurements. The elevated temperature is essential for the optimum functionality of the rigid sensors.

It is evident that the flexible ZnO/PDMS sensor exhibits superior sensing speed, recovery and sensitivity compared to the rigid ZnO/silicon sensor.[S1] The superiority of the flexible ZnO/PDMS sensor can be attributed to: (i) the highly gas permeable nature of PDMS especially towards hydrogen,[S2] and (ii) the unique micro-tectonic morphology of the ZnO on PDMS, as demonstrated in our previous work.[S3] Both these factors result in an increased exposed surface area that reacts with the sensing gas.

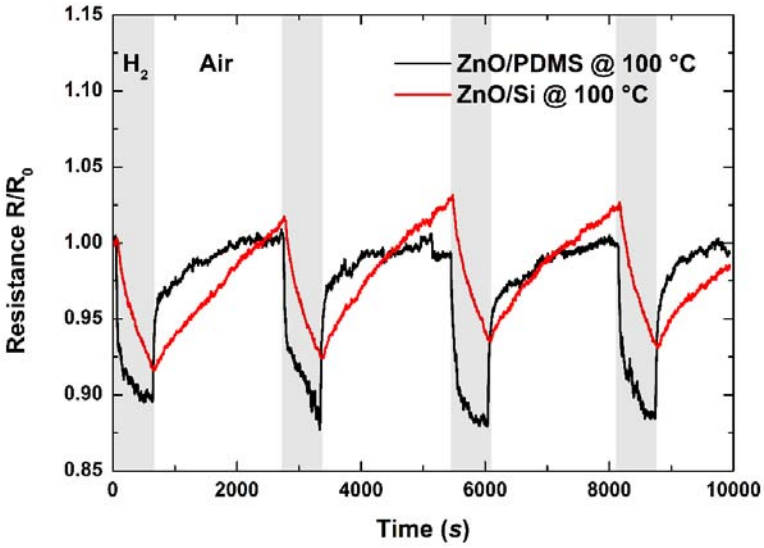


**Figure S1.** Comparison of hydrogen sensitivity of a flexible micro-tectonic (ZnO/PDMS) gas sensor with a rigid analog (ZnO/silicon) at an elevated temperature (100 °C).

**Scanning electron microscopy**

To compare the surface of the ZnO films on polyimide, PDMS and silicon, scanning electron microscopy was carried out using a FEI Nova with a field emission gun source. The silicon and polyimide samples were imaged under high vacuum, while the PDMS sample was imaged in a low vacuum mode at a pressure of 0.6 Torr (**Fig. S2**). It is seen that the film surface is rougher when deposited on the elastomeric substrates. To further verify this observation, a line segment on each surface was profiled to investigate the macroscopic surface roughness. The surface profile along these segments was performed using an Ambios XP-2 surface profilometer (**Fig. S3**). It is clearly seen that the surface roughness is considerably higher on the elastic materials (polyimide and PDMS) which concurs with the observation made using the SEM images. As such, the increased surface area (owing to a higher surface roughness) on the elastomeric substrates leads to better sensing performance, as illustrated in the manuscript.

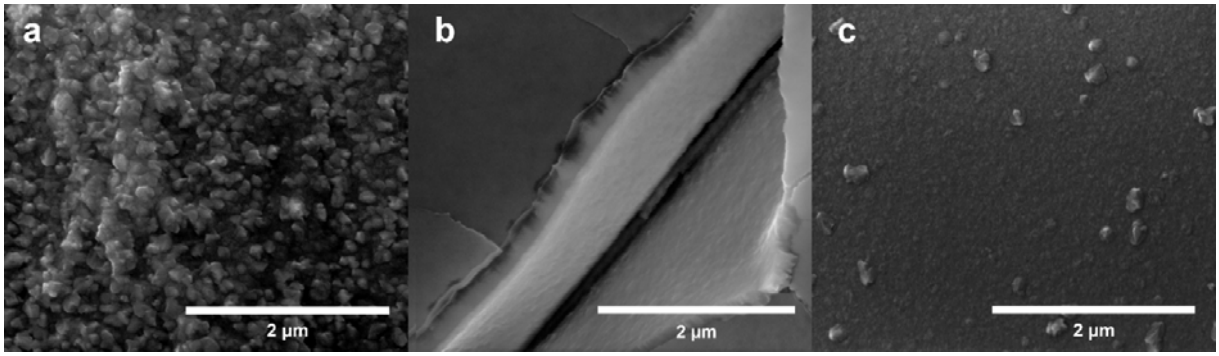


**Figure S2.** Comparison of the ZnO thin film surface of: (a) polyimide, (b) PDMS, and (c) silicon.

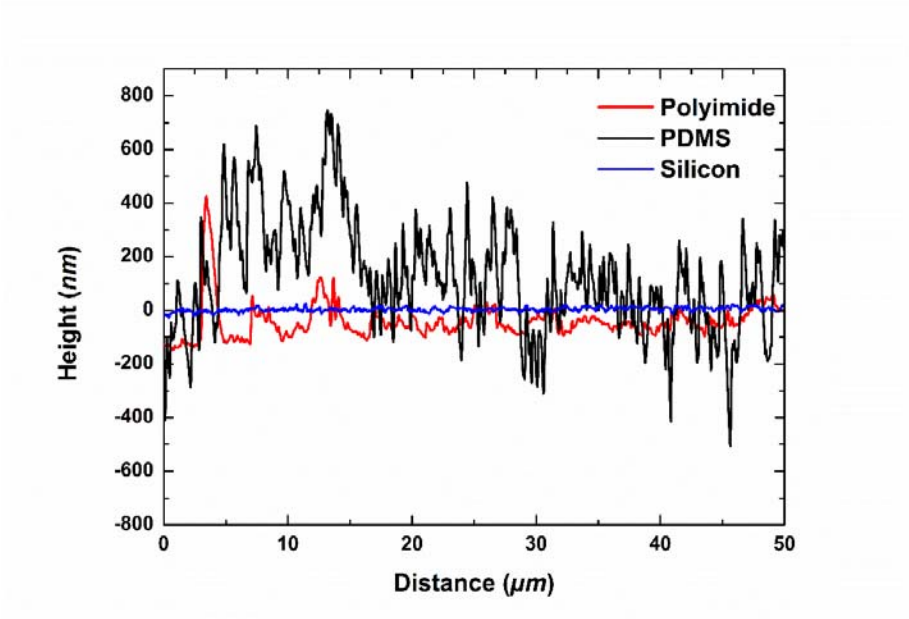


**Figure S3.** Comparison of the ZnO thin film surface on: (a) polyimide, (b) PDMS, and (c) silicon.

**Ultimate UV response of micro-tectonic PDMS sensor**

In the main manuscript, we have shown recovery times of one minute for the ZnO/PDMS sensor before it was exposed again to UV light. When given a longer recovery time, the ZnO film exhibits even larger sensitivity. **Figure S4** shows the normalised change in resistance after a preceding recovery period of 15 min with a following exposure of 48 s. OFF/ON ratios of 100 for the unencapsulated sensor and 18 for the encapsulated sensor can be observed. The increased ON/OFF ratio of the sensors is due to a longer recovery time, which leads to a

higher adsorption of oxygen, resulting in a larger resistance. In case of the encapsulated sensor, the adsorption is slowed down by the PDMS which results in a relatively smaller increase in resistance.

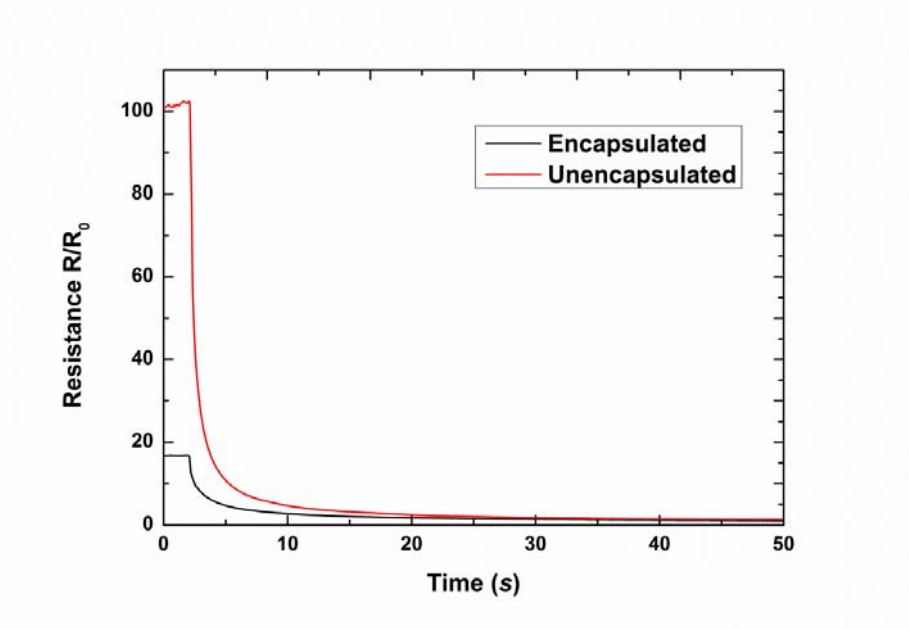


**Figure S4.** Sensor response to UV exposure (48 s) after a preceding long recovery period (15 min).

**X-ray diffraction measurements**

ZnO thin films on polyimide, PDMS and silicon were characterized by X-ray diffraction (XRD) using a Bruker D4 Endeavour diffractometer with a copper *K*α source under identical conditions to determine their crystallographic structure (**Fig. S5**). ZnO thin film deposited on silicon and polyimide substrates show a strongly textured with a dominant (002) orientation. ZnO thin films transferred to PDMS also show a strong (002) orientation. No significant peak broadening and/or shift were observed for the transferred thin film on PDMS in comparison to the directly deposited films on Silicon and Polyimide. These results clearly illustrate that the crystal structure of ZnO thin films is not altered by the transfer process or deposition onto polyimide substrates. This analysis has been performed to eliminate the possibility of any role

played by alterations in crystallinity, on the performance of the sensors. This ensures the validity of a direct comparison between the sensors.

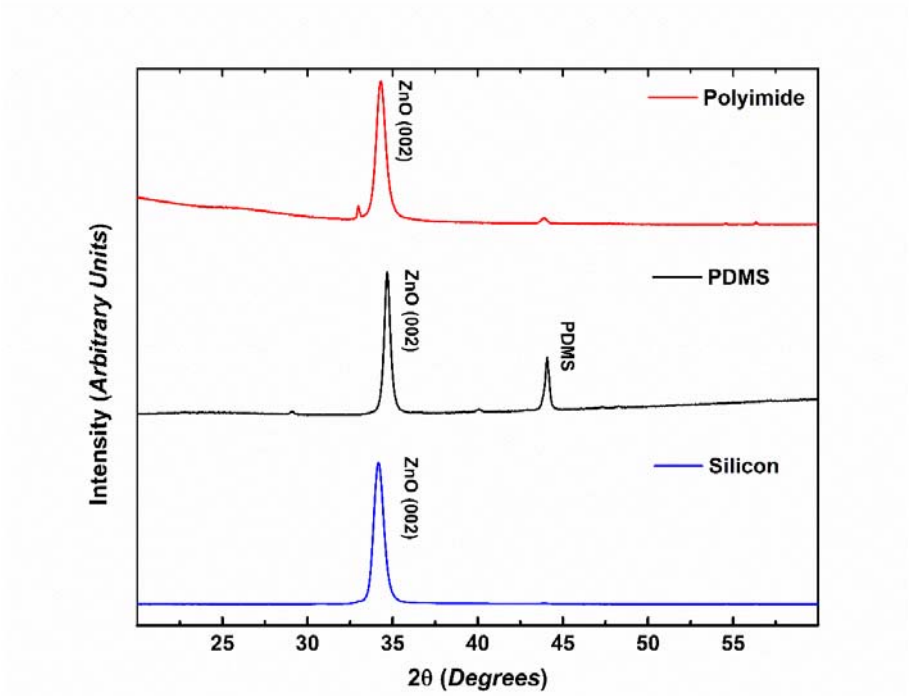


**Figure S5.** XRD of oxygen-deficient ZnO films grown on polyimide, PDMS, and silicon.

**Temperature dependent photosensitivity measurements**

In order to eliminate the role of any stress induced by the elastomeric substrate on performance, a temperature dependent photosensitivity measurement was carried out. The experiment was conducted at room temperature, 100 °C, and 150 °C. This is important to confirm that the increase in sensitivity on elastomeric platforms in comparison to the rigid films is largely governed by the surface topography. The PDMS based ZnO sensor was placed on a temperature controlled stage (Linkam HFS600E-P with a Linkam T95-PE controller). The result depicted in **Fig. S6** show only a slight variation in sensitivity and no change in the response parameters.

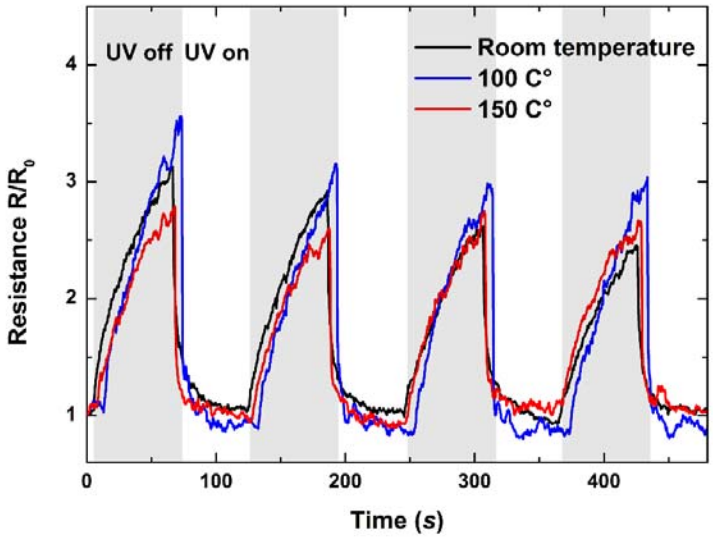


**Figure S6.** Response to UV exposure of ZnO on PDMS sensors at room temperature and at elevated temperature. The sensors were then subjected to UV light with a 1 min exposure followed by 1 min darkness.

**UV transmission measurement**

To determine the absorption wavelength range of the ZnO film and therefore the spectral sensitivity of the sensor, a transmission measurement was performed. The measurement was taken using a Craic PV20/30 micro-photospectrometer with an uncoated PDMS as reference. **Figure S7** shows a clear absorption range between 290 nm to 400 nm, benchmarking the spectral sensitivity of the UV sensor.

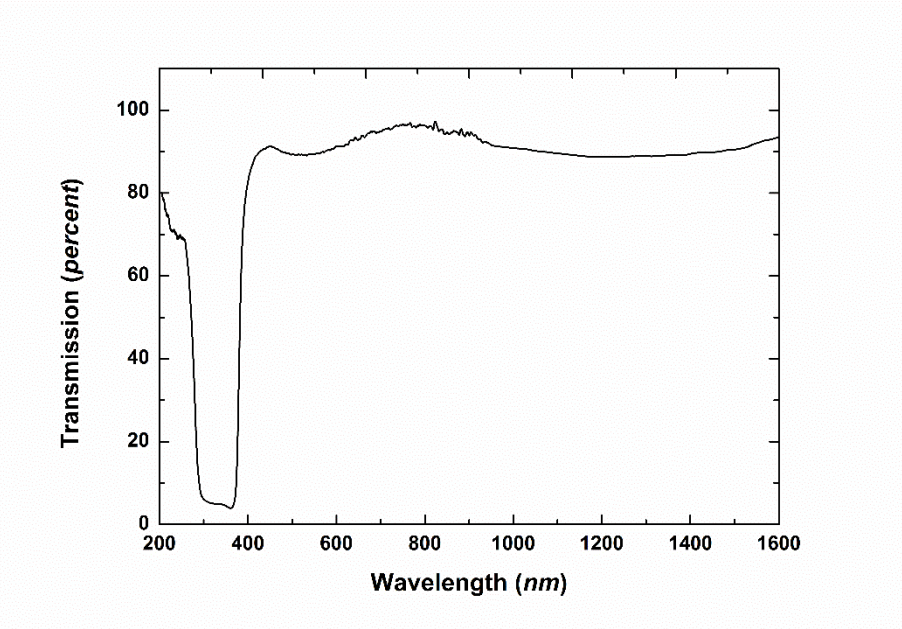


**Figure S7.** Transmission characteristics of oxygen-deficient ZnO thin film on PDMS.

## Verification of oxygen deficiency

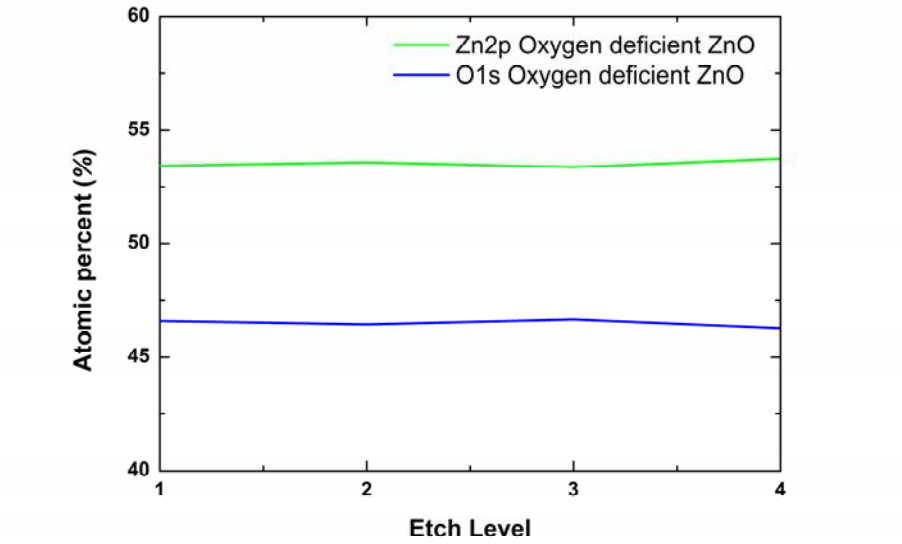


**Figure S8.** XPS analysis of the oxygen-deficient thin films used in this investigation.

To ensure that the sputtered films are oxygen deficient and therefore exhibit the desired gas sensing and UV sensing capabilities, X-ray photoelectron spectroscopy (XPS) was carried out.

The results displayed in **Fig. S8** shows oxygen deficiency throughout the entire thickness of the film.

**Determination of dominant laser wavelength**

For an accurate measurement of the diffraction angle, it is crucial to exactly determine the dominant laser wavelength. Therefore, spectroscopy was performed on both lasers used in the experiments. **Figure S9** shows the dominant intensity peaks which indicate the dominant wavelength of ($\lambda$ = 543.5 nm) for the green He-Ne laser (Uniphase 1974P) and ($\lambda$ = 668.3 nm) for the red diode laser (Thorlabs LDM670).

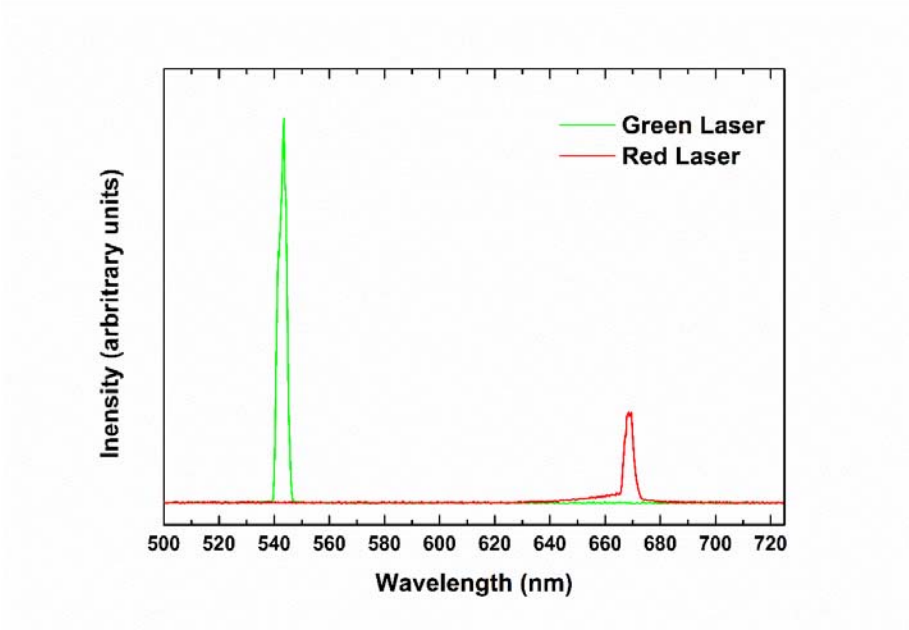


**Figure S9.** Spectrum of the red diode laser and the green He-Ne laser.

**First order diffraction angle determination**

In **Fig. S10**, we show the images that were taken by a Canon 550d mounted on the optical bench in the optical axis of the laser beam. The reference rings on the screen were calibrated before the measurement to ensure dimensional accuracy. Artefacts can be seen around the y

axis on the screen, which are caused by the PDMS surface due to the laser not being focussed on the grating, to ensure a planar wave entering the grating.

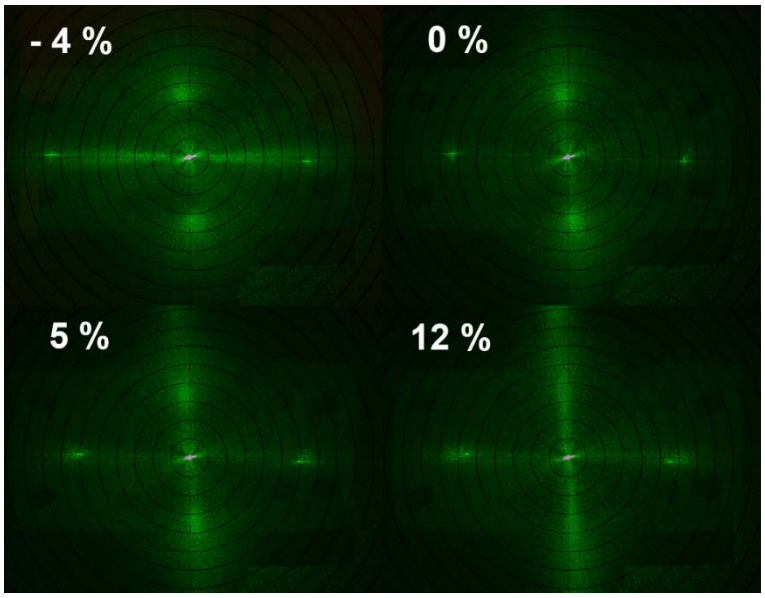


**Figure S10.** Image of the back of the semi-transparent screen used to determine the distance from the zero order centerpoint.

**ZnO thin film DC sputtering conditions**

An oxygen ratio of 40% in the process gas results in crystalline ZnO thin films with almost stoichiometric elemental concentrations through their thickness. At an oxygen ratio of 15%, the O/Zn ratio drops to ~46% yielding oxygen deficient ZnO films. While stoichiometric ZnO films show an almost fully insulating behaviour, the conductivity of the ZnO films increases with decreasing the oxygen partial pressure. This can be ascribed to the presence of oxygen vacancies which act as n-type dopants in ZnO lattice.[S4-S6] The key sputtering parameters are summarised in **Table S1**.

**Table S1.** Sputtering conditions for ZnO thin films

| | |
|---|---|
| Substrate | Pt/Si |
| Target | Zn |
| Process Gas | 15% oxygen in argon |
| Base pressure | $1\times10^{-7}$ Torr |
| Sputtering Pressure | $5\times10^{-3}$ Torr |
| Substrate Temperature | 250 °C |
| DC Power | 200 W |
| Sputtering Rate | 8.5 nm/min |

**Response speed comparison**

In order to compare the performance of the devices on substrates with increasing roughness we measured the response speed of the UV sensors to the broadband radiation (**Table S2**). The ON and OFF speed was measured with respect to the silicon based sensor, which is the device with the lowest sensitivity. The sensors were considered ON and OFF when reaching a resistance change ($R/R_0$) of 0.4.

**Table S2.** Comparison of ON and OFF speeds for UV photosensitivity

| Substrate | OFF Speed (s) | ON Speed (s) |
|---|---|---|
| ZnO on Silicon | 3.5 | 3.0 |
| ZnO on Polyimide | 9.0 | 2.0 |
| Micro-tectonic ZnO on Si | 7.0 | 1.5 |

## References


S1. Bie, L.-J., Yan, X.-N., Yin, J., Duan, Y.-Q. & Yuan, Z.-H. Nanopillar ZnO gas sensor for hydrogen and ethanol. *Sensors and Actuators B: Chemical* **126,** 604-608 (2007).

S2. Rezakazemi, M., Shahidi, K. & Mohammadi, T. Hydrogen separation and purification using crosslinkable PDMS/zeolite: A nanoparticles mixed matrix membranes. *International Journal of Hydrogen Energy* **37,** 14576-14589 (2012).

S3. Gutruf, P. *et al.* Transparent functional oxide stretchable electronics: micro-tectonics enabled high strain electrodes. *NPG Asia Materials* **5,** e62 (2013).

S4. Kappertz, O., Drese, R., Ngaruiya, J. M. & Wuttig, M. Reactive sputter deposition of zinc oxide: Employing resputtering effects to tailor film properties. *Thin Solid Films* **484,** 64-67 (2005).

S5. Zhang, D. *et al.* Properties of ZnO thin films deposited by DC reactive magnetron sputtering under different plasma power. *Appl. Phys. A* **97,** 437-441 (2009).

S6. Xu, Y., Goto, M., Kato, R., Tanaka, Y. & Kagawa, Y. Thermal conductivity of ZnO thin film produced by reactive sputtering. *Journal of Applied Physics* **111,** 084320 (2012).

## 7.7 Supplementary Information for Chapter 6.1

ADVANCED OPTICAL MATERIALS

# Supporting Information

for *Advanced Optical Materials*, DOI: 10.1002/adom.201500346

# Mechanically Tunable High Refractive-Index Contrast $TiO_2$–PDMS Gratings

*Philipp Gutruf,* Eike Zeller, Sumeet Walia, Sharath Sriram, and Madhu Bhaskaran**

Submitted to ADVANCED OPTICAL MATERIALS

## Supporting Information

for *Adv. Opt. Mater.*, DOI: 10.1002/adom.201500346

# Mechanically Tunable High Refractive Index Contrast $TiO_2$–PDMS Gratings

*Philipp Gutruf,* Eike Zeller, Sumeet Walia, Sharath Sriram, and Madhu Bhaskaran**

Functional Materials and Microsystems Research Group & Micro Nano Research Facility, RMIT University, Melbourne, Victoria (Australia)

### Photographs of Diffractions Patterns Collected *In Situ*

In this study, a semi-transparent screen was used to determine the distance between the zero and first order diffraction maxima (denoted as *a* in Equation 1). The distance *a* is then used to calculate the change in the grating period. **Figure S1** shows the photographs of the semi-transparent screen at four representational strains, for both wavelengths (red and green) used in this work. The reference rings seen in Figure S1 were calibrated to minimize measurement errors.

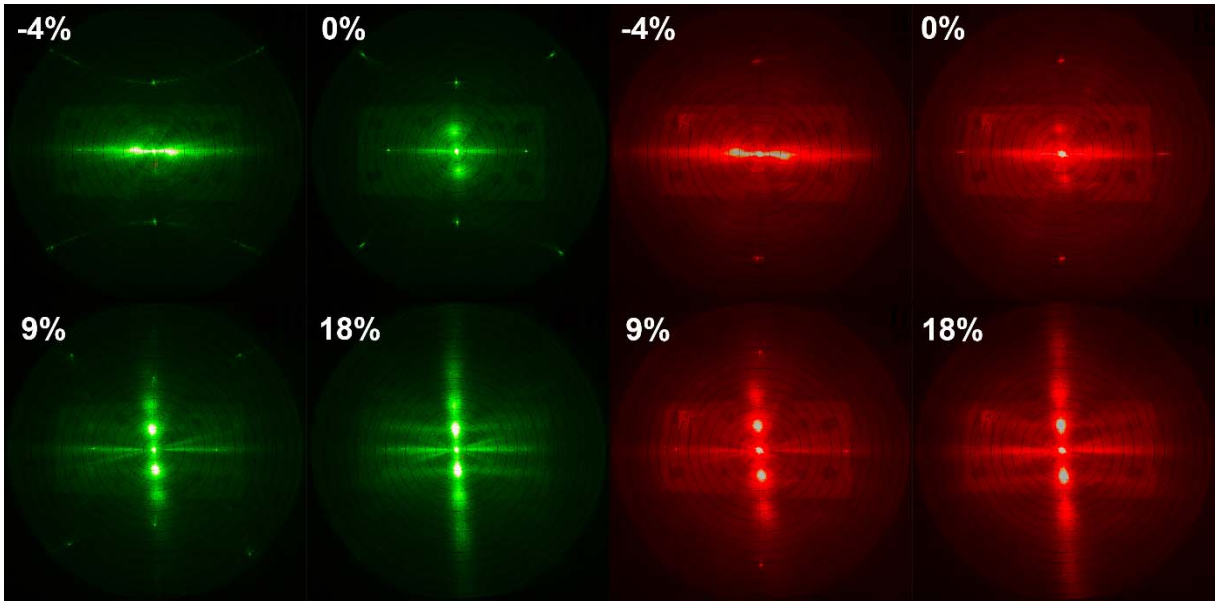


**Figure S1.** Photographs of the semi-transparent screen used to measure the distance between the zero and first order diffraction maxima. Four diffraction patterns at representative strain values are presented for both the green (on the *left*) and the red (on the *right*) lasers.

**Baseline Simulation of Blank Elastomeric Substrate**

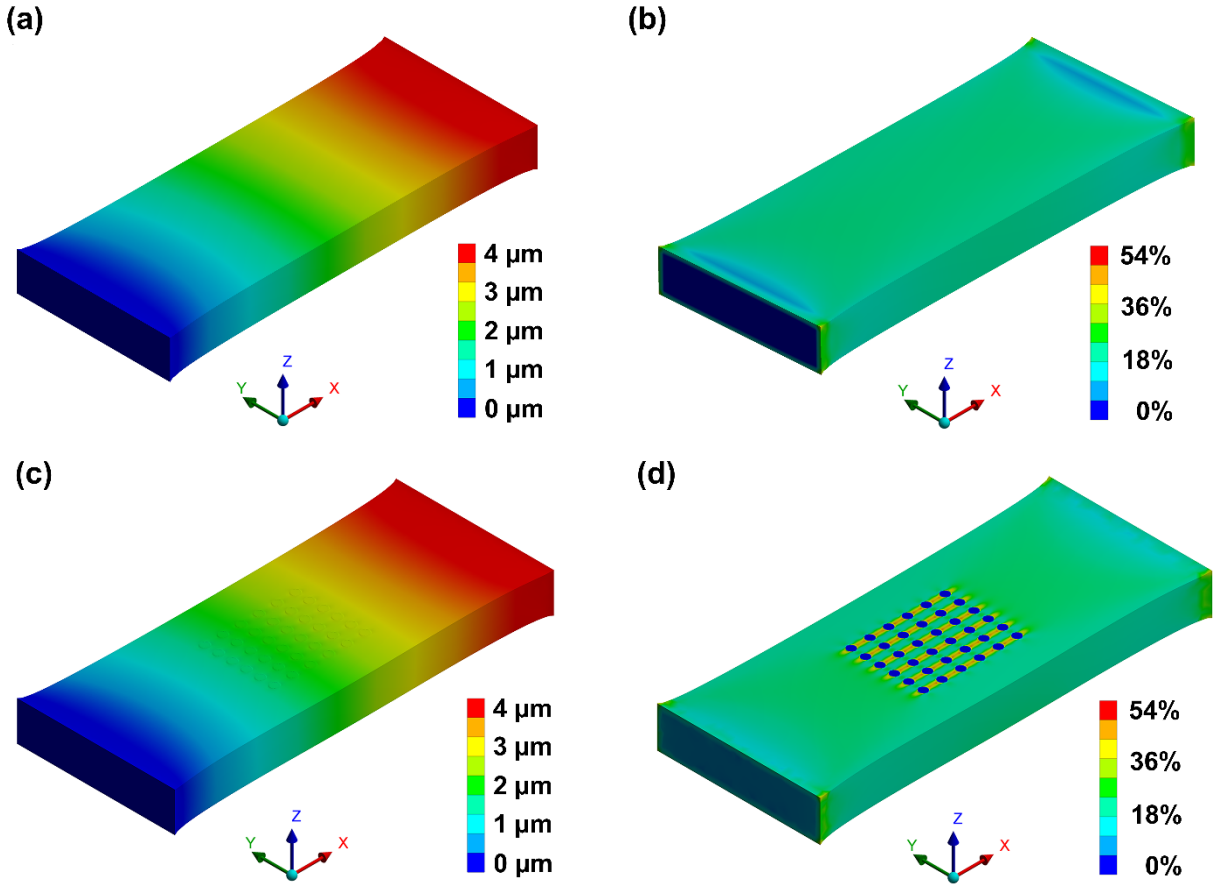


**Figure S2.** Finite element modelling results comparing (**a**,**b**) pure/blank PDMS with (**c**,**d**) $TiO_2$-embedded PDMS. Three-dimensional map of deformation for an applied strain of 20% (4 µm displacement) in the X direction for sample clamped at one end are shown in (**a**) and (**c**). Three-dimensional map of strain distribution (normalized) under condition are shown in (**b**) and (**d**).

In order to establish a baseline, we simulated a blank PDMS substrate to compare with the $TiO_2$-embedded PDMS presented in the article. Identical analysis methods for the total deformation normalized strain of a blank PDMS substrate were used. The blank PDMS substrate was subjected to identical deformation (of 4 µm), which is equivalent to 20% strain. **Figure S2**a shows a map of the total deformation and Figure S2b the normalized strain, with the direct comparison to the $TiO_2$-embedded PDMS presented in Figures S2c and S2d. It should

be noted that Figures S2c and S2d are the same as Figures 4b and 4c. When compared to the grating counterpart it is evident that the grating has only minimal impact of the deformation and strain occurring in the PDMS substrate.

**Refractive Index Characterization**

As the refractive index of oxide thin films depends on the synthesis method, we performed characterization in the visible light regime. In order to determine the refractive index of the $TiO_2$ thin film used in this article, we used a Filmetrics F40 system (system based on spectral reflectance). The obtained results are consistent with literature[S1] and offer a high refractive index contrast to PDMS.[S2]

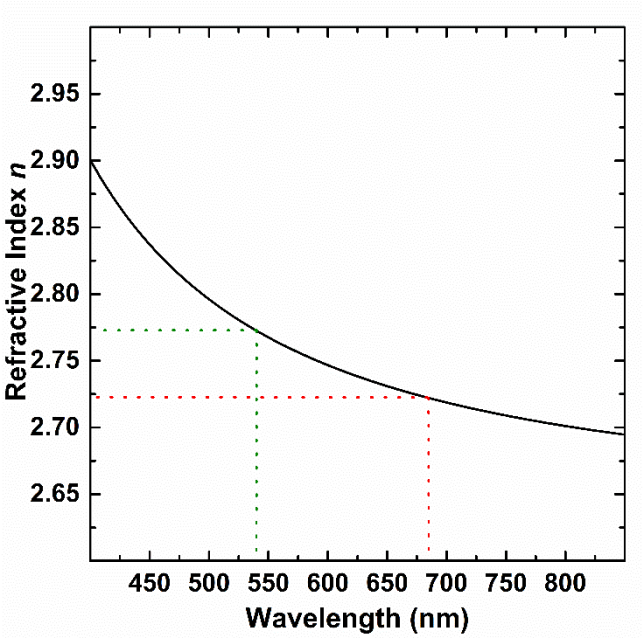


**Figure S3.** Refractive index of the $TiO_2$ thin films synthesized by electron beam evaporation. The refractive index for the relevant wavelengths (green at 543.5 nm and red at 668.3 nm) are indicated.

In order to assess the effect of strain on the refractive index and its subsequent effect on the device, we measured the refractive index under varying degrees of strain. For this purpose, a custom made stretching stage was used to strain the PDMS films in a Filmetrics F40 system. Only minimal change in refractive index is observed even under 50% strain. This shows that the effect of change of refractive index is negligible on the functionality of the device.

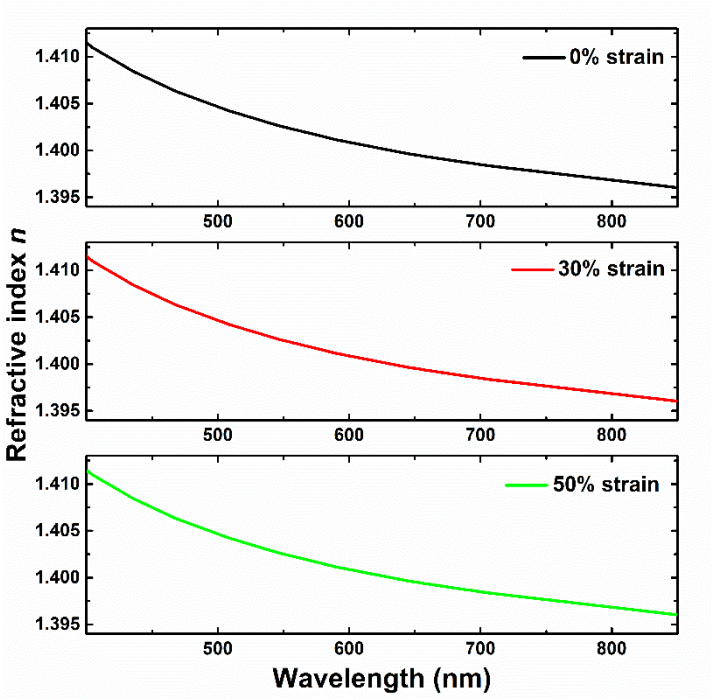


**Figure S4.** *In situ* refractive index change with strain increasing from 0 to 50%.

**References**

[S1] M. Suhail, G. M. Rao, S. Mohan, *J. Appl. Phys.* **1992**, *71*, 1421-1427.

[S2] S. Motakef, T. Suratwala, R. Roncome, J. Boulton, G. Teowee, D. Uhlmann, *J. Non-Cryst. Solids* **1994**, *178*, 37-43.

## 7.8 Supplementary Information for Chapter 6.2

# Supporting Information for: Mechanically Tunable Dielectric Resonator Metasurfaces at Visible Frequencies

*Philipp Gutruf,*[†,‡,#] *Chengjun Zou,*[§,#] *Withawat, Withayachumnankul,*[§,ǁ] *Madhu Bhaskaran,*[†,‡] *Sharath Sriram,*[†,‡] *and Christophe Fumeaux*[*,§]

[†]Functional Material and Microsystems Research Group, RMIT University, Melbourne, Victoria, Australia, [‡]Micro Nano Research Facility, RMIT University, Melbourne, Victoria, Australia, [§]School of Electrical and Electronic Engineering, The University of Adelaide, South Australia 5005, Australia, and [ǁ]Interdisciplinary Graduate School of Science and Engineering, Tokyo Institute of Technology, Ookayama, Merguro-ku, Tokyo 152-8552, Japan.

[#]P.G. and C.Z. contributed equally.

[*]Address correspondence to christophe.fumeaux@adelaide.edu.au

## Simulation of strain-dependent lattice deformation

Mechanical simulations were undertaken by finite element modelling (FEM) to evaluate deformation of the oxide–elastomer composite structure. The FEM was carried out using the ANSYS 15 Mechanical tool.

The geometric parameters were defined with the polydimethylsiloxane (PDMS) substrate being 10 μm × 5 μm × 1.5 μm, with the 6×6 array of dielectric resonators centred on and embedded in the PDMS substrate. The materials properties used for PDMS were: Young's modulus of 20 MPa,[S1] density of 965 kg m$^{-3}$,[S2] and Poisson's ratio of 0.40,[S3] The $TiO_2$ dielectric cylinders embedded in the PDMS are 190 nm in diameter and 102 nm thick, with Young's modulus of $1.4\times10^6$ MPa,[S4] density of 4,260 kg m$^{-3}$,[S5] and Poisson's ratio of 0.28,[S6] The 6×6 dielectric resonator array has 408 μm period in both the *x* and *y* directions. The geometric constraints and iteration steps are chosen to ensure manageable simulation

complexity. Figure S1 shows the mechanical simulated unit cell deformations along the *x*- and *y*-directions upon application of uniaxial strain along the *x*-direction.

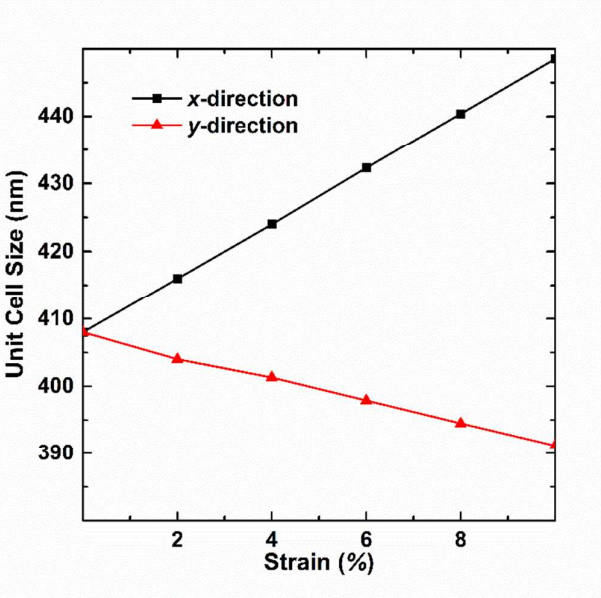


**Figure S1.** Simulation of change in unit cell period upon application of strain along the *x*-direction.

In order to evaluate the influence of dielectric resonators embedded in PDMS, a blank substrate was compared to the dielectric-embedded structure. The results are presented in Figure S2, with identical deformation analysis performed in both cases (elongation of 0.6 µm, equivalent to 6% strain). Direct comparison of the total deformation (Figure S2a-c) and normalised strain (Figure S2b-d) shows that the dielectric resonators do not impact the deformation of the PDMS substrate.

It should be noted that Figure S2c-d are the same as Figure 4a-b in the main manuscript.

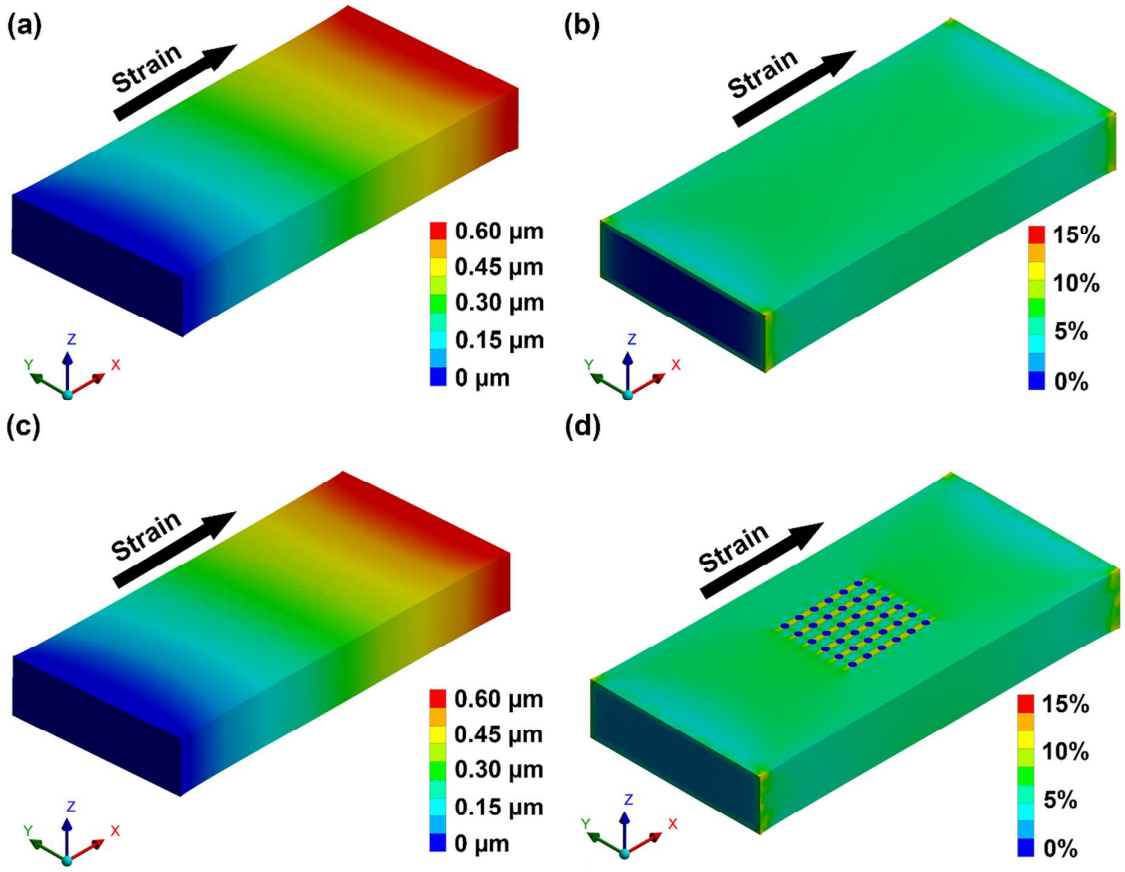


**Figure S2.** Finite element modelling results. Results for 6% applied strain on (a,b) blank PDMS substrate and (c,d) PDMS substrate with embedded dielectric resonators. Three-dimensional maps of total deformation are shown in (a) and (c), with normalised strain shown in (b) and (d).

## References


S1 Bowden, N.; Brittain, S.; Evans, A. G.; Hutchinson, J. W.; Whitesides, G. M. Spontaneous Formation of Ordered Structures in Thin Films of Metals Supported on An Elastomeric Polymer. *Nature* **1998**, *393*, 146-149.

S2 Nisar, A.; Afzulpurkar, N.; Mahaisavariya, B.; Tuantranont, A. Multifield Analysis Using Multiple Code Coupling of a MEMS Based Micropump with Biocompatible Membrane Materials for Biomedical Applications. in *BioMedical Engineering and Informatics, 2008. BMEI 2008. International Conference on.* **2008**, *1*, 531-535.

S3 Xia, Y.; Kim, E.; Zhao, X.-M.; Rogers, J. A.; Prentiss, M.; Whitesides, G. M. Complex Optical Surfaces Formed by Replica Molding Against Elastomeric Masters. *Science* **1996**, *273*, 347-349.

S4 Ottermann, C.; Kuschnereit, R.; Anderson, O.; Hess, P.; Bange, K. Young's Modulus and Density of Thin $TiO_2$ Films Produced by Different Methods, *Mater. Res. Soc.* **1996**. *436*, 251–256.

S5 Reddy, M.; Rao, V. V.; Reddy, B.; Sarada, S. N.; Ramesh, L. Thermal Conductivity Measurements of Ethylene Glycol Water Based $TiO_2$ Nanofluids. *Nanosci. Nanotechnol. Lett.* **2012**, *4*, 105-109.

S6 Mayo, M.; Siegel, R.; Narayanasamy, A.; Nix, W. Mechanical Properties of Nanophase $TiO_2$ As Determined by Nanoindentation. *J. Mater. Res.* **1990**, *5*, 1073-1082.